N72 32691

NASA CR-112144

QUASI-STEADY PLASMA ACCELERATORS

by

A. C. Ducati

prepared for

NATIONAL AERONAUTICS AND SPACE ADMINISTRATION

Contract NAS 1-10630

Plasmadyne
a division of GEOTEL, INC.
Santa Ana, California

NASA CR-112144

Report FR-062-10630

QUASI-STEADY PLASMA ACCELERATORS

by

A. C. Ducati

prepared for

NATIONAL AERONAUTICS AND SPACE ADMINISTRATION
Langley Research Center
Hampton, Virginia 23365

Contract NAS 1-10630

June 1972

Plasmadyne
a division of GEOTEL, INC.
Santa Ana, California

FOREWORD

This is the report on work carried out during the period of 5 April 1971 to 5 June 1972 by Plasmadyne, a division of Geotel, Inc., on "Quasi-Steady Plasma Accelerators," Contract NAS 1-10630, originating in the Environmental and Space Sciences Division, Langley Research Center, Hampton, Virginia, under the direction of James M. Hoell, Jr.

Adriano C. Ducati was the Principal Investigator in charge of the work. Robert G. Jahn collaborated as a consultant; F. A. Block, R. J. Bregozzo, A. O. Jones, S. E. Killops and W. A. Stanfill participated in the conduction of the experiments; and Willis Stoner contributed to the preparation of the report.

ABSTRACT

Results are reported from a continued study of MPD thrusters operating in the quasi-steady mode and using electrode vapor as the propellant. Testing methods have been refined, and performance data is now available for a fairly wide range of thruster geometries. Performance was found to be strongly dependent on thruster geometry, with some designs showing approximately twice the efficiency obtained during the preceding contract period reported in Reference 1. The radial clearance between electrodes, the attachment point of the arc on the cathode, and the electrical resistance of the electrodes appear to be important design variables. As a result of the availability of reliable test data, the program is entering a rapid learning phase which could lead to further improvements in performance. The report presents test results, an analysis of these results, and recommendations for continued work in the area.

TABLE OF CONTENTS

LIST OF ILLUSTRATIONS

LIST OF ILLUSTRATIONS (continued)

1.0 INTRODUCTION

This report describes work performed under Contract NAS 1-10630 for the study of arc thrusters operating in the quasi-steady mode and using electrode vapor as the propellant. The activity is a continuation of work started under Contract NAS 1-10140 and reported in Reference 1. The type of thruster being evaluated is believed to be potentially capable of the good performance associated with large, high powered MPD thrusters without requiring a large power source and without encountering the intense heating problems that go with steady operation at high powers. Furthermore, the use of consumable electrodes introduces propellant directly into the most intense portion of the arc at precisely the time of the arc discharge. Electrodes are cooled ablatively, which reduces thermal stresses, and they can be renewed by a feeding mechanism. However, some difficult problems must be solved to realize these advantages. Perhaps the most complex is to find a configuration that has low losses and at the same time is suitable for electrode feeding. When these difficulties are overcome, the result is expected to be a thruster design that is exceptionally simple and provides high performance and good reliability for long operating periods.

The work reported in Reference 1 was largely concerned with getting the thrust producing system and the test facility working properly so that meaningful data could be obtained. When complete performance data became available, results were quite limited and were considered preliminary. These early tests showed that specific impulse in an attractive range could be obtained with propellant supplied purely by ablation; however, the arc impedance and the efficiency were found to be quite low for the preliminary thruster designs. The tests demonstrated that the newly developed test equipment for generating the electrical discharge, for measuring impulse, and for installing or removing a thruster from the torsional pendulum could be made to work satisfactorily. They also showed that a test chamber pressure of 10^{-6} torr or less can be maintained while operating a pulsed thruster having consumable graphite electrodes. Difficulties uncovered included problems in the design of graphite electrodes with low resistive losses, problems in measuring the change in electrode weight with sufficient accuracy, and problems associated with triggering the arc with a high voltage pulse. A considerable amount of work was done on the arc triggering problem which led to the design of a low voltage contact-type system which has proved to be a workable concept.

In the present report period, the emphasis has shifted with more time spent on refining measurement techniques and accumulating test data on a wider range of designs. Enough data are now available to provide criteria for improving the thruster designs, and initial efforts have resulted in a substantial increase in efficiency and further improvement in the reliability of the triggering system. However, further refinements of the test methods are needed and a large quantity of work remains to be done for understanding the operation of the arc, improving the performance of the thruster, and developing a design with long life and practical arrangement for feeding the electrodes.

This report presents recent test results, examines these results in an effort to establish the cause of losses and other performance deficiencies, and describes changes being made in the propulsion system to improve its performance. The reader is referred to References 1 and 2 for a detailed description of the test facility and of the propulsion system geometry used when the present program was initiated.

2.0 EXPERIMENTAL RESULTS

2.1 Improvements in the Test Facility

The test procedure is a time-consuming one when electrode vapor is used as the source of propellant. To obtain a single test point a thruster must be carefully weighed, installed in the vacuum chamber, operated for a series of identical pulses, and finally removed from the test chamber for reweighing. A remotely-controlled manipulator for installing and removing thrusters from the torsional pendulum without releasing the vacuum in the test chamber was developed in an earlier phase of this program, and its initial use was reported in Reference 1. Since that time, improvements have been made in the system, and its use is now permitting test data to be obtained at a much faster rate.

The initial design of the thruster mounting device encountered difficulty in achieving satisfactory electrical conduction in the contacts for the main arc discharge. A cam action was used to clamp the contact surfaces, and the action was found to be somewhat inadequate. The problem was remedied by using the two thruster mounting bolts to clamp flat surfaces together to complete the main arc discharge circuit. This arrangement has been working without difficulty. In addition, provision was made for seven light leads by engaging seven spring-loaded contacts with a cam action. These leads are used for the triggering discharge, the triggering solenoid, and any instrumentation leads that are required.

Figure 1 is a general view of the end of the test chamber showing the installation probe entering the chamber through its sliding seal. The manipulating knobs are visible at the far right in the photograph. A separate valved port below and to the left of the main one allows thrusters to be introduced into the chamber for test when impulse measurements are not required. The rack in the foreground holds alternate installation probes on which thrusters can be installed in readiness for a quick change between series of tests.

Figure 2 is a closer view of the end of the probe showing a thruster about to enter the sliding seal of the main valved port. To install a thruster on the torsional pendulum, it is clamped to the probe using the center manipulator rod, and the probe is inserted into the valved port until the seal engages. Slack is then taken up in the cable and winch that controls movement of the probe, and the valve is opened. The torsional pendulum is now locked in a fixed position using a remotely-actuated clamping device, and the vacuum is allowed to draw the probe into the chamber as the winch releases more cable. Figures 3, 4 and 5 show the thruster approaching the mounting plate, and finally passing through the opening in the plate and seating in position in Figure 6. The three outer manipulator rods are next used to tighten the mounting bolts and turn the cam that engages the seven spring-loaded contacts. When this is complete, the center rod is used to release the probe from the thruster, and the probe is withdrawn from the test chamber by the winch (Figures 7 and 8). Finally, the torsional pendulum can be unclamped and the test series started.

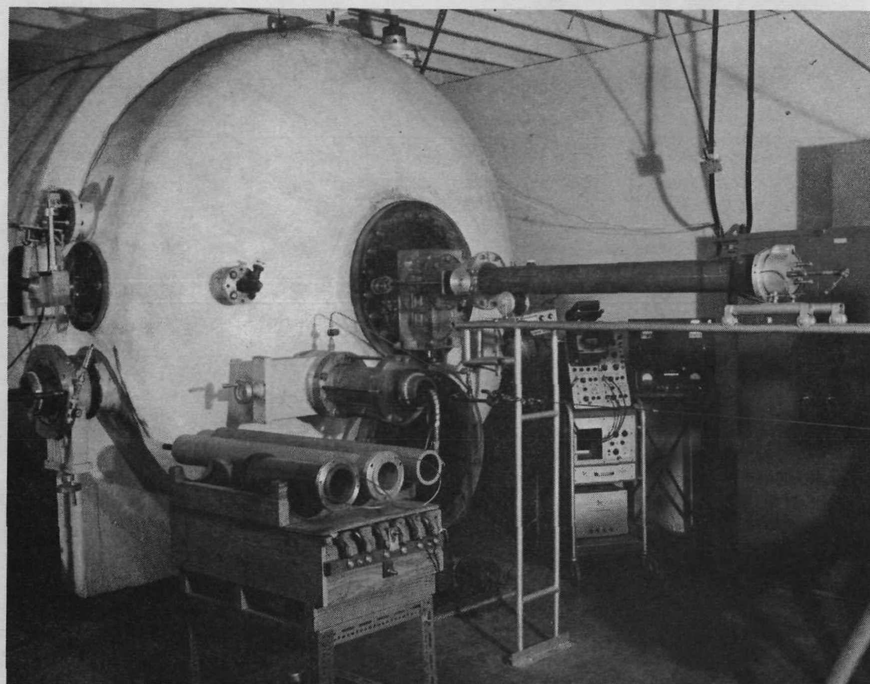

Figure 1. End of the Test Chamber Showing the Installation Probe in Position to Enter the Chamber

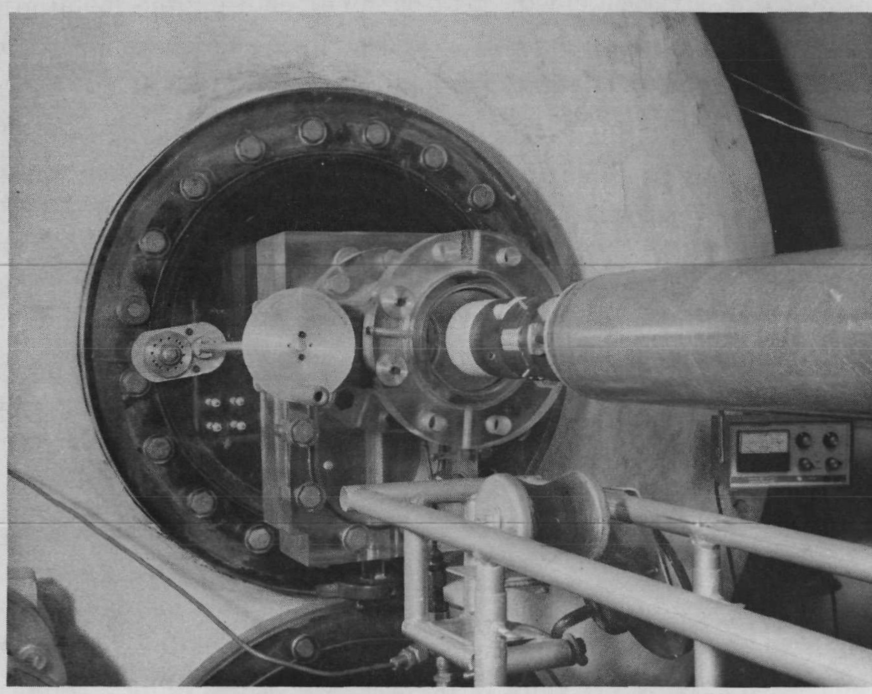

Figure 2. Thruster Mounted on the Installation Probe Ready to Enter the Test Chamber Through the Valved Port

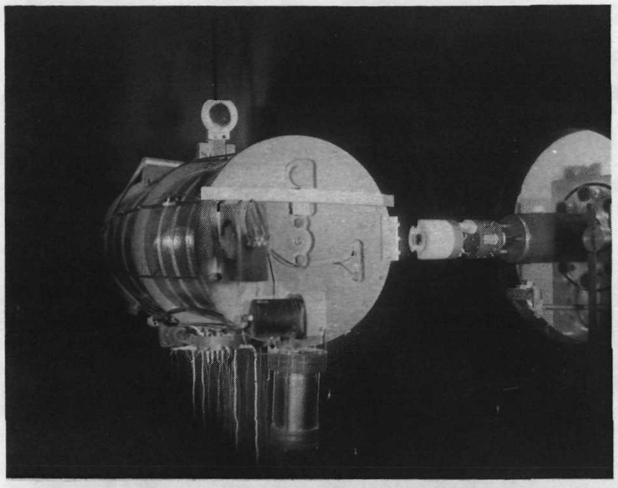

Figure 3

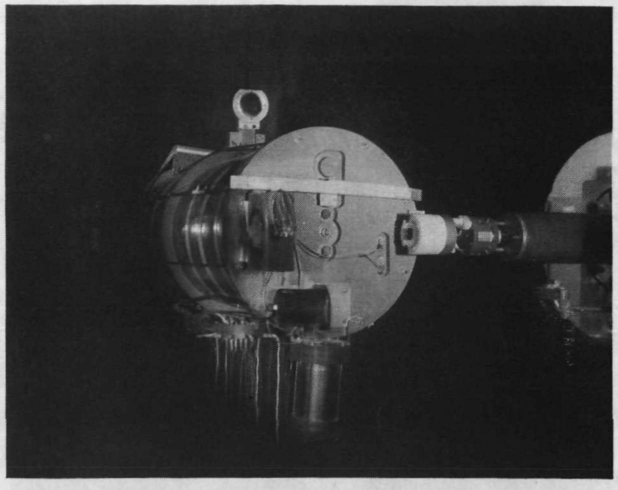

Figure 4

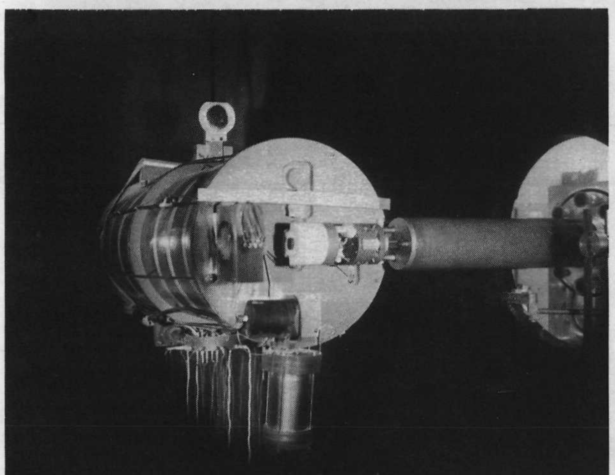

Figure 5

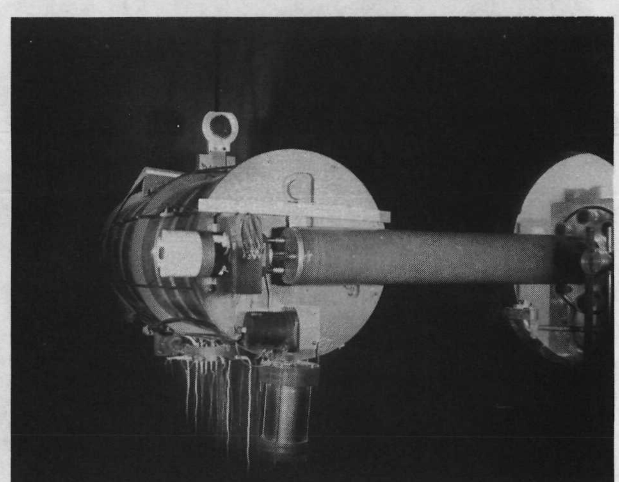

Figure 6

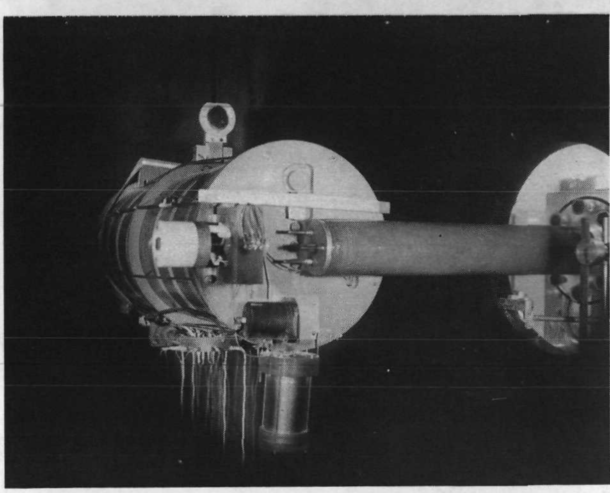

Figure 7

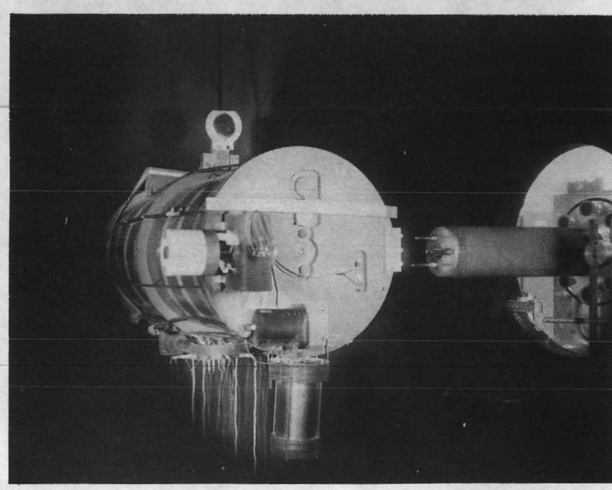

Figure 8

Figures 3 - 8. Installation Probe Moving the Thruster Into and Out Of Operating Position on the Torsional Pendulum

Figure 9 shows the side of the test chamber. The large windows of medium height provide a side view of the thruster when it is mounted on the torsional pendulum and are also used for a view through a telescope of the graduated scale that measures pendulum deflection. The index line for the scale is projected through the upper window. The lower window provides a side view of the thruster when it is operating attached to a probe in the lower of the two valved ports. This is the position used for most photographic work. A separate program (being conducted under AFOSR Contract F44620-70-C-0002) is concerned with details of the arc behavior and is making use of photographic techniques to help establish the arc geometry. For this purpose a second window at the lower level, but located further downstream, has been equipped with an extension tube and a 90-degree reflecting prism to provide a view looking directly upstream into the arc chamber. By photographing a discharge through these two windows, a correlation is obtained between the geometry of the arc and the appearance of the plume.

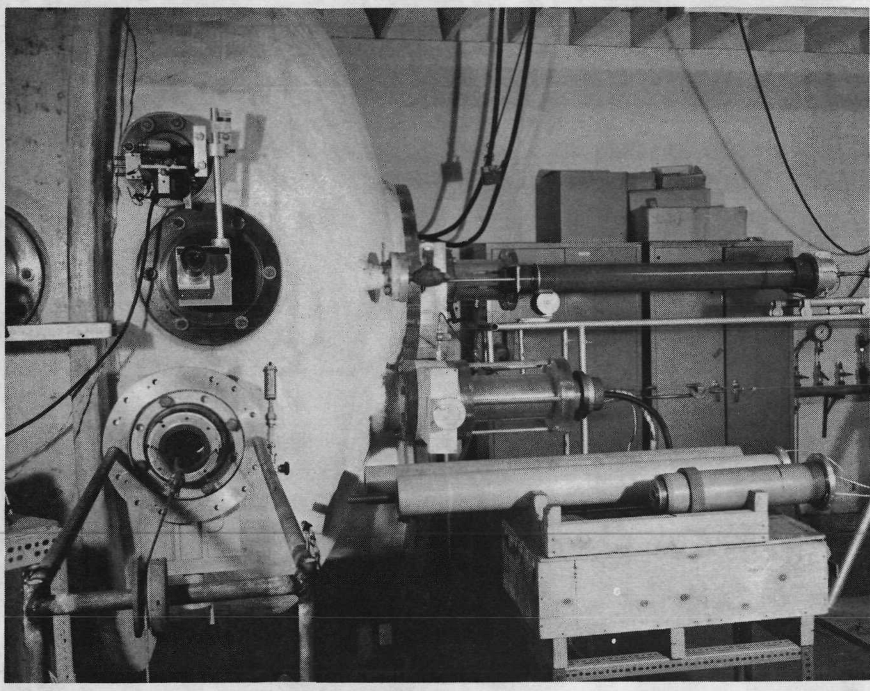

Figure 9. Side View of the Test Chamber

2.2 Improved Measurement Techniques

The testing of pulsed thrusters requires that a great deal of care be taken to assure that the measurements are of satisfactory accuracy. The three quantities that must be measured to determine overall performance are the electrical energy delivered to the thruster during a pulse, the average amount of material consumed as propellant during a pulse, and the total impulse developed during the pulse. All three have required careful study and the development of special equipment to obtain satisfactory data. A number of desired improvements are still not complete.

Probably the most straightforward measurements are those used to determine the electrical energy expended during a pulse. A special coaxial shunt and coaxial leads are used to pick up arc current and arc voltage signals. Electrical energy is determined by numerical integration of the arc power during the complete discharge. The system described in Reference 1 has been found to be satisfactory and is still in use. Nevertheless, some unexpected noise signals have been encountered and eliminated, and questions remain unanswered regarding the significance of using the complete integrated pulse energy as opposed to using a reduced energy more representative of the quasi-steady portion of the discharge.

The measurement of the mass of material consumed as propellant has been particularly troublesome. Propellant is obtained from vaporization of the electrodes and adjoining insulating material, so it is necessary to carefully weigh these parts before and after a series of pulses to determine the amount of material expended during the test. The normal procedure is to disassemble the thruster and weigh the critical parts separately so that the contribution of each may be determined. The thruster is then installed on the ballistic pendulum and operated for fifty identical pulses while performance measurements are made. A second weighing then establishes the change in mass. Figures 10 and 11 show arc chamber parts disassembled for weighing. From left to right in Figure 10 the parts shown are the anode, the cathode, and the triggering electrode, all of graphite, and a disc insulator of boron nitride. Some thruster designs also include a ring insulator such as is shown in Figure 11. Typical values for the total change in mass fall between 0.5 and 2.0 milligrams per pulse or between 25 and 100 milligrams for each test series. A weight error of 1.0 milligram for each part therefore introduces errors of several percent in the total mass change figures. These errors can be reduced by using a more precise balance or by increasing the number of pulses in a series. However, there are other possible errors that have not been fully evaluated. These include weight changes in parts of the thruster that are not weighed, and sorption of moisture and other impurities by the graphite electrodes and insulating materials. A strong effort is being made to resolve these questions, and this work is taking priority over continued thruster improvement based on present measurement techniques.

Arc discharges to the brass parts in which the electrodes are clamped and to the external body of the thruster have occasionally been observed, and can result in a change in the weight of the parts involved. These are not normal operating modes, but weighing of more parts may be necessary to detect their occurrence. It is interesting to note that parts can gain as well as lose weight. This occurs when cool surfaces are exposed to gas in the arc chamber. Carbon deposits are easily observed on white insulator surfaces and

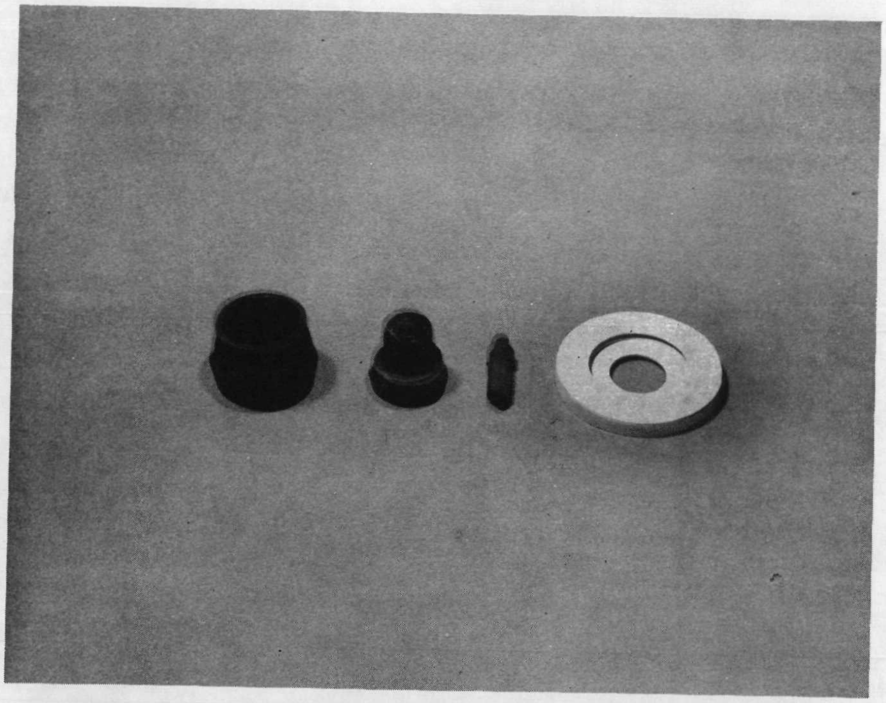

Figure 10

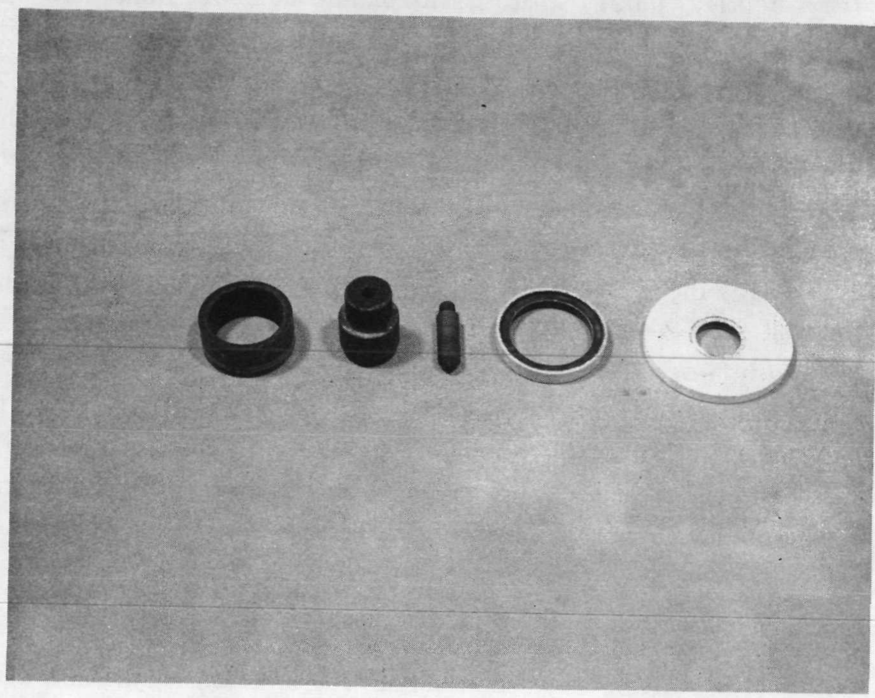

Figure 11

Figures 10 - 11. Arc Chamber Parts Disassembled for Weighing sometimes result in an increase rather than a decrease in insulator weight. Care must be taken in the insulator design to avoid the formation of a complete conducting path between electrodes. Carbon deposits on the anode have a dull or soft appearance that can be distinguished from the normal arc erosion. Some anode designs increase in weight while others decrease, and it is conceivable that the weight of parts farther from the arc may be affected by carbon deposits.

To detect weight changes in unexpected locations it would be desirable to weigh the complete thruster as well as the arc chamber parts. There are several precision balances on the market that can handle units weighing as much as 1.0 kilogram with a sensitivity of 0.1 milligram. Under carefully controlled conditions, the change in weight could be determined with an error no greater than a few milligrams which would be satisfactory provided the other part of the problem which is the sorption of moisture and other impurities by the thruster parts can be solved.

When a thruster is removed from the vacuum chamber after a test series, it has been operating at high temperature and at a pressure of around 10^{-6} torr and is presumably well outgassed. If it could be weighed immediately each time, the weight difference obtained would probably be accurate. An exception could occur if a film of vacuum oil accumulates on cooler parts of the thruster due to backstreaming from the diffusion pump; but improved forepumping has essentially eliminated all evidence of backstreaming in the system, and any remaining deposits on the arc chamber parts would be boiled off by the high temperature operation and should present no problem if the thruster is removed using the remotely operated manipulator before it cools completely. However, errors became evident very early in the program, particularly in the graphite parts, due to the sorption of moisture and possibly other impurities as the thruster cools while being disassembled and before being weighed. The hygroscopic properties of carbon products vary over a wide range depending on the purity and porosity of the material. The International Critical Tables(3) show values of water content by weight varying from 6 percent for carbon black on a humid day to less than 1.0 percent for foundry coke. Notice, however, that even 0.1 percent moisture by weight in the electrodes would represent an error which is a large fraction of the total weight change being measured in some test runs. A satisfactory solution to this problem will therefore require extreme care. Dushman(4) notes that the sorptive capacity of graphite is considerably less than that of charcoal with most grades of material. Our own experience is that a 5.0-gram graphite part will typically increase in weight about 0.05 percent during exposure to the atmosphere at room temperature (compared to a total weight change of about 0.30 percent during a test series). This amount of uncertainty is unacceptable, particularly since the error tends to be additive if all parts are weighed under the same conditions.

In the initial test series reported in Reference 1, it was found necessary to desiccate the samples and immediately transfer them to the analytical balance. Questions remained, however, regarding the consistency of the desiccator treatment, and it has been replaced by a vacuum oven which is used to dry the parts before weighing. This is an interim measure that has been used for the test series described in this report. Parts are dried in a Blue M Model SV-56A, 300-watt vacuum oven which can hold a part at a temperature above 160°C while the chamber is evacuated by a small mechanical vacuum pump. After drying, vacuum is released by the introduction of dry nitrogen. The parts are then weighed using a Mettler Type H15 analytical balance which can be read to the nearest 0.1 milligram. The balance is equipped with an external basket supported by a wire which extends into the vacuum chamber through an opening in its top. This permits weight to be determined without removing the part from the vacuum oven. A plug which closes the opening for the wire while the furnace is evacuated is removed while the weight is taken. The vacuum oven and the analytical balance are shown in Figure 12. The method is considered an interim one because the weighing is done at atmospheric pressure. It is desired to reduce weighing errors to no more than one part in 10,000 so the effects of buoyancy and

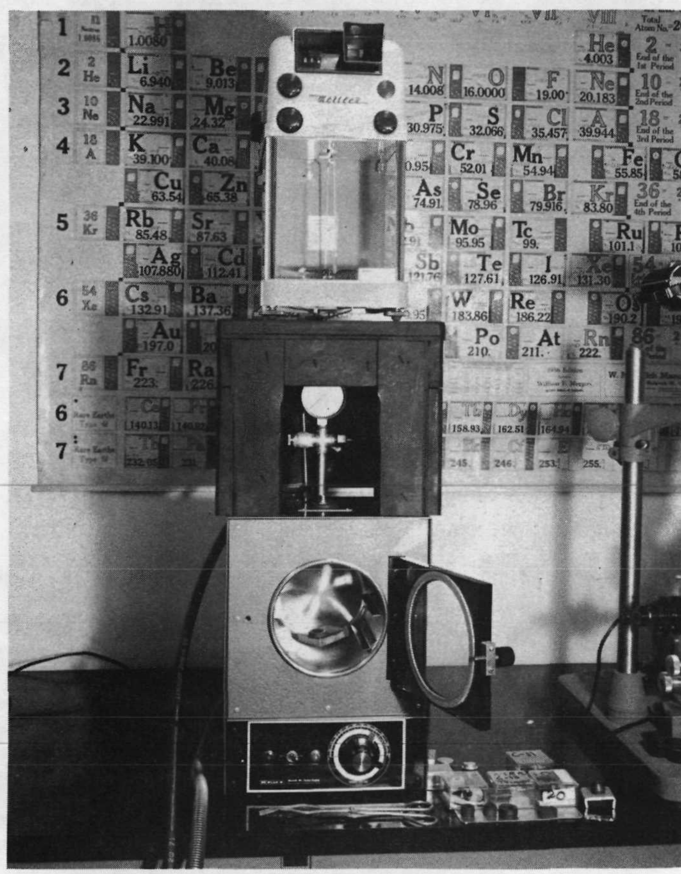

Figure 12. Setup of Vacuum Oven and Balance Used for Drying and Weighing Arc Chamber Parts

convection currents while the parts are hot can be important. On the other hand, if the parts are allowed to cool completely before weighing, they could conceivably pick up some moisture again. In the most extreme case visualized, the buoyancy error would be no more than 1.0 milligram for a 5.0-gram graphite part. Although undesirable, this much error would be considered acceptable. However, the errors due to correction currents which occur when cool gas is introduced to release the vacuum can be more serious. Gas heated by the oven walls tends to rise, causing a downdraft in the center of the chamber where the part is suspended. The importance of this effect is difficult to estimate, but from observed changes in the reading following release of the vacuum, it is believed to amount to around 2.0 milligrams. For five parts, each weighed two times, with a probable error of 2.0 milligrams, the probable error for the total mass change would be $\sqrt{10\,(2\text{ mg})^2} =$ 6.3 milligrams. On a percentage basis, this amounts to a probable error of 12 or 13 percent for a typical series of 50 pulses having a total mass change of 50 milligrams. To remove this source of error, the development of a vacuum weighing system has been undertaken in parallel with the test program.

A vacuum weighing system that is capable of weighing the electrodes and insulators separately is nearing completion and is shown in Figure 13. The instrument consists of two small evacuated chambers connected by a slender tube. The weighing pan, which is

Figure 13. System Being Developed for Drying and Weighing Arc Chamber Parts in a Continuous Vacuum

located in the lower chamber, is suspended by a fine wire from a load cell in the upper chamber. The sample to be weighed is heated to a temperature between 100°C and 150°C by a focused beam from a tungsten filament outside of the chamber while the enclosure is evacuated. The load cell consists of a Statham Model UC3 Universal Transducing Cell equipped with a Model UL5 Micro-Scale accessory. The accessory is a linkage that magnifies the force acting on the strain gage by a factor of ten. The result is a nominal full scale range of 6 grams (which can be exceeded appreciably before hitting the stops) and a nominal nonlinearity and hysteresis limit of 9 milligrams. It has been found, however, that the hysteresis alone is a small fraction of this value. By using a standard weight of nearly the same mass as the sample and weighing one after the other, the difference in mass between the two can be determined and has been found to repeat within 1.0 milligram. By comparing the sample weight to the standard weight before and after each test series it should be possible to measure the weight change of the sample with an error in the neighborhood of 1.0 milligram which is considered acceptable, at least for test series of 100 pulses or more. Externally controlled manipulators for removing the sample from the pan and replacing it with the standard weight without releasing the vacuum are being constructed.

It is believed that the techniques described will essentially eliminate systematic errors in the mass change measurements. As an example of the accuracy expected from the system, consider a case with five parts, each weighed with a random probable error of 1.0 milligram. Each part is weighed before and after the test series, so ten measurements are involved, giving a probable error for the total mass change of:

$$\text{probable error} = \sqrt{10\ (1\ \text{mg})^2} = 3.2\ \text{mg}$$

For a typical series of 100 pulses, the total mass change is around 100 milligrams, so the probable error for the total mass change can be expected to be 3 or 4 percent.

The above method is considered most suitable for the measurements of the mass change of individual electrodes and insulators. A method for weighing the complete thruster in a vacuum oven remains to be developed and will be undertaken next making use of experience gained from use of the smaller vacuum weighing unit. It is planned in the meantime to conduct tests of the accuracy of the system by weighing sample parts not included in the thruster assembly before and after a test series. These parts would be mounted on a probe and introduced into the test chamber environment through an instrumentation port. Zero weight change for these samples would confirm the accuracy of the vacuum weighing technique and eliminate questions regarding effects such as vacuum oil backstreaming.

The accurate measurement of propellant mass used from consumable electrodes and other thruster parts has been found to be a difficult problem. The accuracy of measurements made in the past is open to some question, but equipment and techniques are now at hand for making measurements of satisfactory accuracy and checking the precision of these measurements.

The torsional pendulum for measuring total impulse was the subject of intense study in earlier phases of this program, and the instrument is presently performing satisfactorily. The technique used does not require the pendulum to be stopped before each shot. Instead, each shot is triggered at the instant that the pendulum swings through its null position, and the total impulse is determined from the change in maximum amplitude with which the pendulum swings. A sample test point record is presented in Figure 14. Test conditions are identified at the top left hand side of the sheet. Below this, the weights of the thruster parts before and after the test series are recorded, and the average weight loss per pulse is determined. This is followed by calibration data for the torsional pendulum and a determination of the total impulse and specific impulse from the average change in pendulum swing per pulse and the thruster mass change per pulse. A sample oscilloscope trace showing arc current and voltage variation during a discharge is attached at the bottom of the sheet. The voltage trace is, of course, the one that drops from a higher value when the discharge is initiated. These traces are not recorded for each pulse in a series, but ten to twenty pictures are normally made to assure repetitive conditions. Pulse energy is found by integrating under a plot of the product of current and voltage for the duration of the discharge, and an average is taken if a difference is found between pulses.

The right hand side of the sheet shows the way the amplitude of the pendulum swings are recorded. The first pulse starts the instrument swinging, and the maximum amplitude is entered in the left hand column labeled "Min." for minutes of arc. The second pulse is applied during the return swing at the null position, and tends to stop the swinging motion. The second amplitude figure for the swing to the opposite side of the scale (which is recorded on the right hand side) is greatly reduced. This pattern of alternately increasing and decreasing amplitude is repeated throughout the series. The impulse introduced by each pulse is proportional to the number entered in the difference (Diff.) column. These figures are plotted on the second page of the data form (Figure 15) so that the uniformity of the data can be judged at a glance. The variation shown in this figure is fairly typical for a thruster that is running for the first time after installation in the test chamber. The first pulse or two usually shows a higher impulse, which is presumed to be due to outgassing as the electrodes are heated. Following an initial fall-off, a gradual increase in impulse is normally observed. The reason for this change has not yet been determined. Possible explanations include reduced thermal losses and improved arc behavior due to a gradual increase in electrode temperature, and improved arc goemetry due to favorable changes in the electrode shape as ablation progresses. Tests have been planned to help in establishing the true explanation.

Figure 16 shows the scale used to measure the deflection of the pendulum. The scale moves with the pendulum. Graduations are on a curved surface at a radius of about

Discharge No. 2844-2894

Year: *1972* Month: *2* Day: *29*
Head No: *20* Volts: *400*
Chamber Pressure: *10 x 10⁻⁷*
Electrode Distance, 10^{-3} in: *125*
Electrode Type and Weight:

	Type *C9*	Before mg	After mg	Diff. mg
+	Anode: *4Al*	*4866.3*	*4860.0*	*6.3*
−	Cath: *6Kl*	*4200.5*	*4175.3*	*25.2*
	Tr: *1T5*	*1238.5*	*1238.7*	*+ 0.2*
	Disk: ◊	*5579.3*	*5553.8*	*25.5*
	Ring: ◊	*2055.9*	*2055.4*	*0.5*
	Total:	*17,940.5*	*17,883.2*	*57.3*
	Total No. Discharges:			*50*
	Δm/Discharge, mg:			*1.146*

◊ *Insulators*

Calibration Force, mg:	*1000*
Time of Application, sec:	*5*
Total Calib. Impulse, mg sec:	*5000*
Total Calib. Deflection, min:	*145*
Sensitivity (S), mg sec/min:	*34.5*
Total Deflection, min:	*4795*
Average Deflection (θ), min:	*96*
I/Discharge = (S x θ), mg sec:	*3312*

Isp = (I/Δm), sec:	*2890*

** This 250-volt pulse was used to bring alternate amplitude readings closer to zero. (not used in data)*

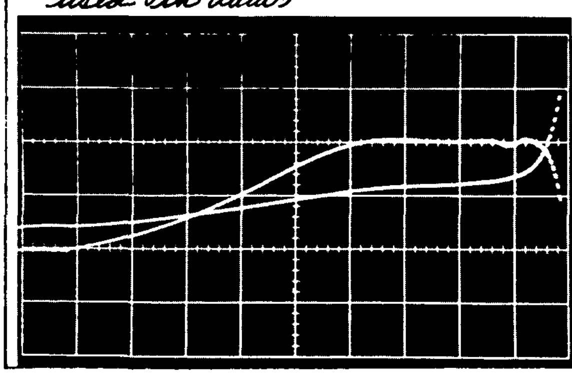

Time H	Time M	+ V	+ Diff.	+ Min.	Discharge No.	− Min.	− Diff.	− V
10	*15*							
						3		
			103	*106*	*2844*			*400*
		400			*2845*	*13*	*93*	
			92	*105*	*2846*			*400*
		400			*2847*	*16*	*89*	
				16				
		* *250*			*2848*	*2*		
			93	*95*	*2849*			*400*
		400			*2850*	*5*	*90*	
			91	*96*	*2851*			*400*
		400			*2852*	*6*	*90*	
			92	*98*	*2853*			*400*
		400			*2854*	*10*	*88*	
			92	*102*	*2855*			*400*
		400			*2856*	*11*	*91*	
			94	*105*	*2857*			*400*
		400			*2858*	*12*	*93*	
			94	*106*	*2859*			*400*
		400			*2860*	*9*	*97*	
			95	*104*	*2861*			*400*
		400			*2862*	*9*	*95*	
			94	*103*	*2863*			*400*
		400			*2864*	*9*	*94*	
			95	*104*	*2865*			*400*
		400			*2866*	*7*	*97*	
			96	*103*	*2867*			*400*
		400			*2868*	*5*	*98*	
			95	*100*	*2869*			*400*
		400			*2870*	*6*	*94*	
			94	*100*	*2871*			*400*
		400			*2872*	*8*	*92*	
			97	*105*	*2873*			*400*
		400			*2874*	*9*	*96*	
			96	*105*	*2875*			*400*
		400			*2876*	*10*	*95*	
			96	*106*	*2877*			*400*
		400			*2878*	*9*	*97*	
			97	*106*	*2879*			*400*
		400			*2880*	*5*	*101*	
			101	*106*	*2881*			*400*
		400			*2882*	*6*	*100*	
			101	*107*	*2883*			*400*
		400			*2884*	*6*	*101*	

Figure 14. Sample Record of Data for a Test Series (First Sheet)

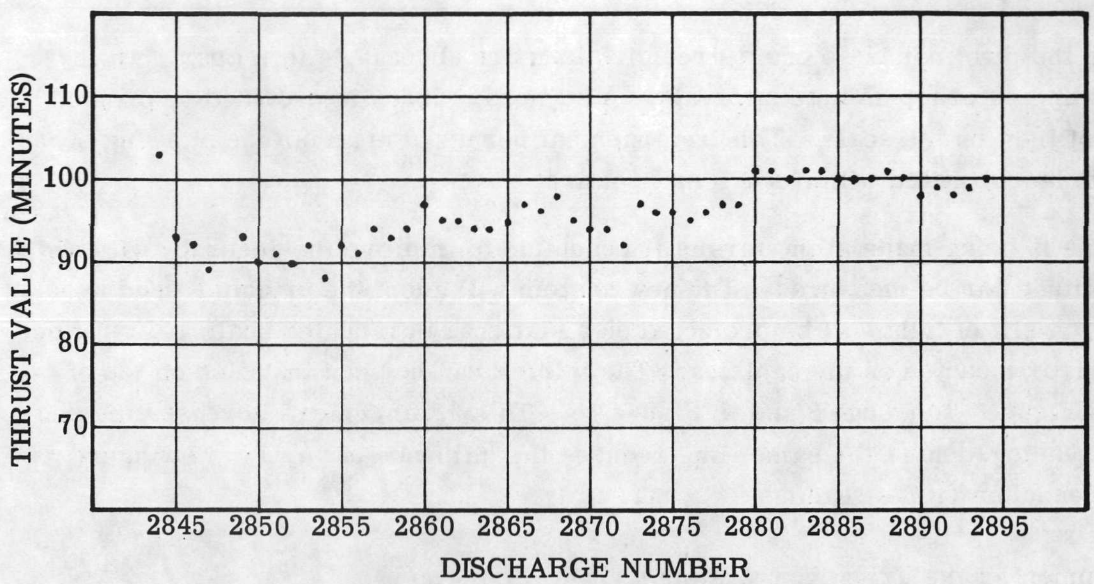

Figure 15. Sample Record of Data for a Test Series (Second Sheet) Showing Impulse Reading as a Function of Discharge Number

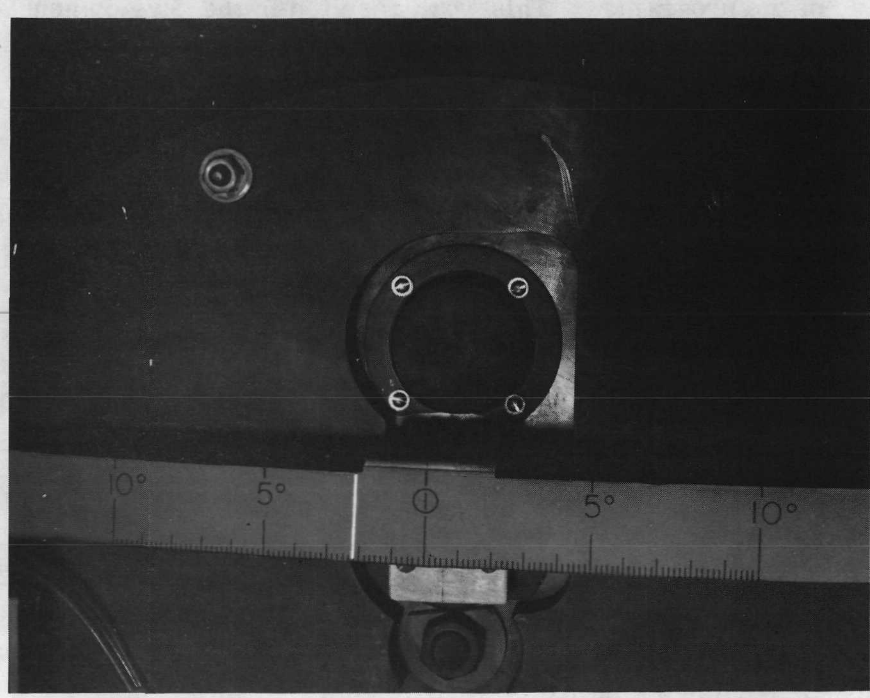

Figure 16. Scale Sector and Index Beam Used to Measure the Deflection of the Torsional Pendulum

25 inches from the pivot point, so one degree divisions are about 0.44 inch apart, while finer divisions appear at ten-minute intervals. A stationary index is provided by projecting a thin slit of light on the scale. This arrangement permits the amplitude of swing of the pendulum to be estimated within one minute of arc.

A change is being made in the torsional pendulum to improve the accuracy with which the swing amplitude can be measured. The new system will adopt the principle used in a galvonometer. A slit of light will be projected on a stationary graduated scale after reflection from a mirror mounted on the canister. The mirror can be seen installed on top of the canister in Figures 3 through 8 and in Figure 16. This arrangement increases the sensitivity of the reading, and at the same time reduces the influence of any axial swinging motion of the pendulum on the reading.

2.3 Development of the Triggering System

The triggering problem is particularly difficult for a vacuum arc because no gas is introduced until the arc is started, which means that a conventional system would require a voltage high enough to initiate an arc under space conditions. Furthermore, there is a tendency for the insulators to become coated with a film of condensed electrode material making it difficult to use a high voltage system. An extensive study of this problem was made in an earlier phase of the program.(1) This work resulted in the development of a contact-type triggering system that operates at low voltage. A separate triggering electrode is used that momentarily contacts one of the main electrodes and forms an arc as the contact opens. The resulting discharge of ionized gas triggers the main arc. A separate small capacitor is used to energize the triggering discharge. This type of system has been found to be much more reliable than the earlier high voltage systems, and to provide better control of the location of the main arc discharge. It is the only type of system being considered in the present studies.

To further alleviate the triggering problem, the main electrodes were designed with an unusually small radial gap. The expectation was that the main arc discharge would start across the small gap, but would quickly be drawn downstream by electromagnetic forces to a more favorable position with the arc attached near the center of the inner electrode. As will be discussed later, this did not occur to the extent that was desired, and it is now believed that a larger radial clearance between electrodes would be advantageous. As a consequence, further improvement of the triggering system has been a high priority activity. A good triggering system would be one that provides reliable starts with a large radial gap between electrodes, thereby permitting improved thruster performance.

A wide range of geometries of contact triggering systems have been evaluated to find which types are most effective. For each design, the charge on the triggering capacitor was progressively reduced until starts were no longer obtained consistently. Designs that start the arc across a large radial gap with a minimum triggering voltage are considered the most satisfactory. Some designs work reliably with only a 50-volt charge on a 1000-microfarad capacitor, while others require as much as 500 volts; so there are large differences between designs.

There are four possible arrangements for the arc chamber obtained by reversing polarity and by making the triggering electrode contact either the anode or cathode. These are illustrated in Figure 17. The main arc electrodes are shown crosshatched, while the triggering electrodes are shown as black dots. The arc is initiated by momentarily touching the triggering electrode to the main electrode of opposite sign. The configuration used most often is the one depicted in the upper left diagram, in which a positive trigger is used to contact a central cathode.

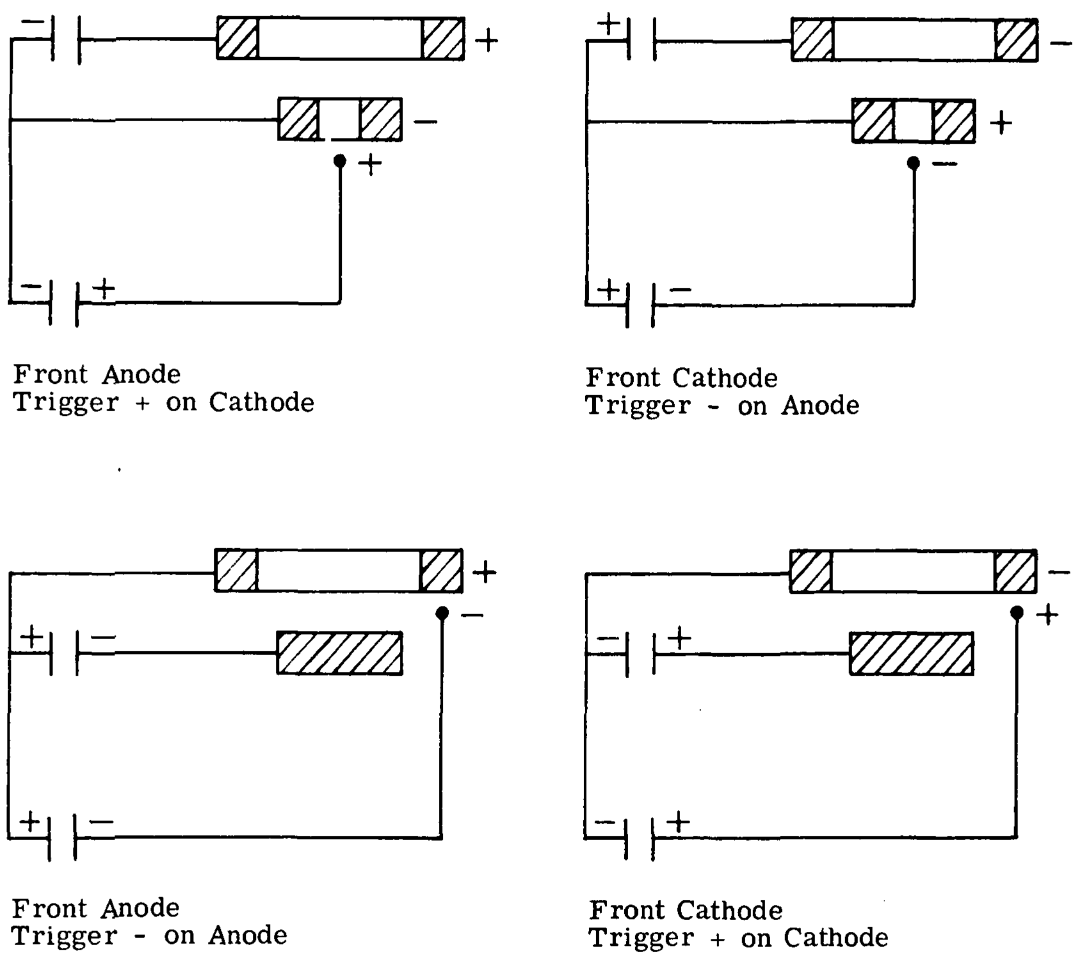

Figure 17. Four Possible Arrangements for the Main Electrodes and the Triggering Electrode

The designs that start most easily with a moderate discharge energy for triggering seem to be those that use the same electrode as the cathode for both the triggering circuit and the main arc discharge. Although the triggering process is a complex one, the observations made can be explained by assuming that the main arc discharge is initiated when a point on the cathode surface becomes hot enough to emit electrons. This is more readily accomplished if the triggering electrode contacts the cathode rather than the anode, as occurs in the upper left and lower right diagrams.

Other variations are obtained by modifying the arrangement of the passage that directs ionized gas from the triggering arc into the gap between electrodes. Some of the geometries tried are shown in Figure 18. So far, these variations seem to have less effect on arc initiation than the polarity of the triggering electrode.

2.4 Thruster Design

Progress has been made both in the details of construction of the thruster and in understanding how the arc behaves and what changes in geometry are needed to improve operation.

Under the first category, the construction of the thruster has been altered in three respects. First, a change in arrangement was necessary to adapt to the new method of mounting on the torsional pendulum. The purpose of the change was to improve the electrical conductivity of the connections for the main power leads as discussed in Section 2.1. Figure 19 shows (from left to right) a view of the original thruster configuration described in Reference 1, the revised thruster configuration (with mounting base) used in the current tests, and an alternate thruster body arranged with the triggering mechanism in the outer electrode. The use of a separate mounting base permits this portion of the assembly to be reused easily when the thruster design is changed. The axial grooves in the sides of the thrusters permit the assemblies to enter the mounting hole on the torsional pendulum which has two protruding elements to take the mounting screws and carry the current for the arc discharge.

Second, a need was discovered for an improved method for clamping the graphite electrodes in the metal fixture that transfers electrical current into the graphite. The designs reported in Reference 1 used conical contact surfaces into which the graphite parts were pressed axially by clamping screws. Inspection of the metal surfaces after operation revealed roughened areas on the polished surfaces as a result of hot spots due to poor electrical contact. The conical surfaces were not matched well enough. This condition was remedied by changing to cylindrical mating surfaces with a split metal ring that clamps on the graphite. It was found that the cylindrical surfaces can be machined with the required accuracy to avoid high resistance in the contact region. The older type of design is shown in Figures 20 and 21, while an example of improved configuration is shown as Figure 22.

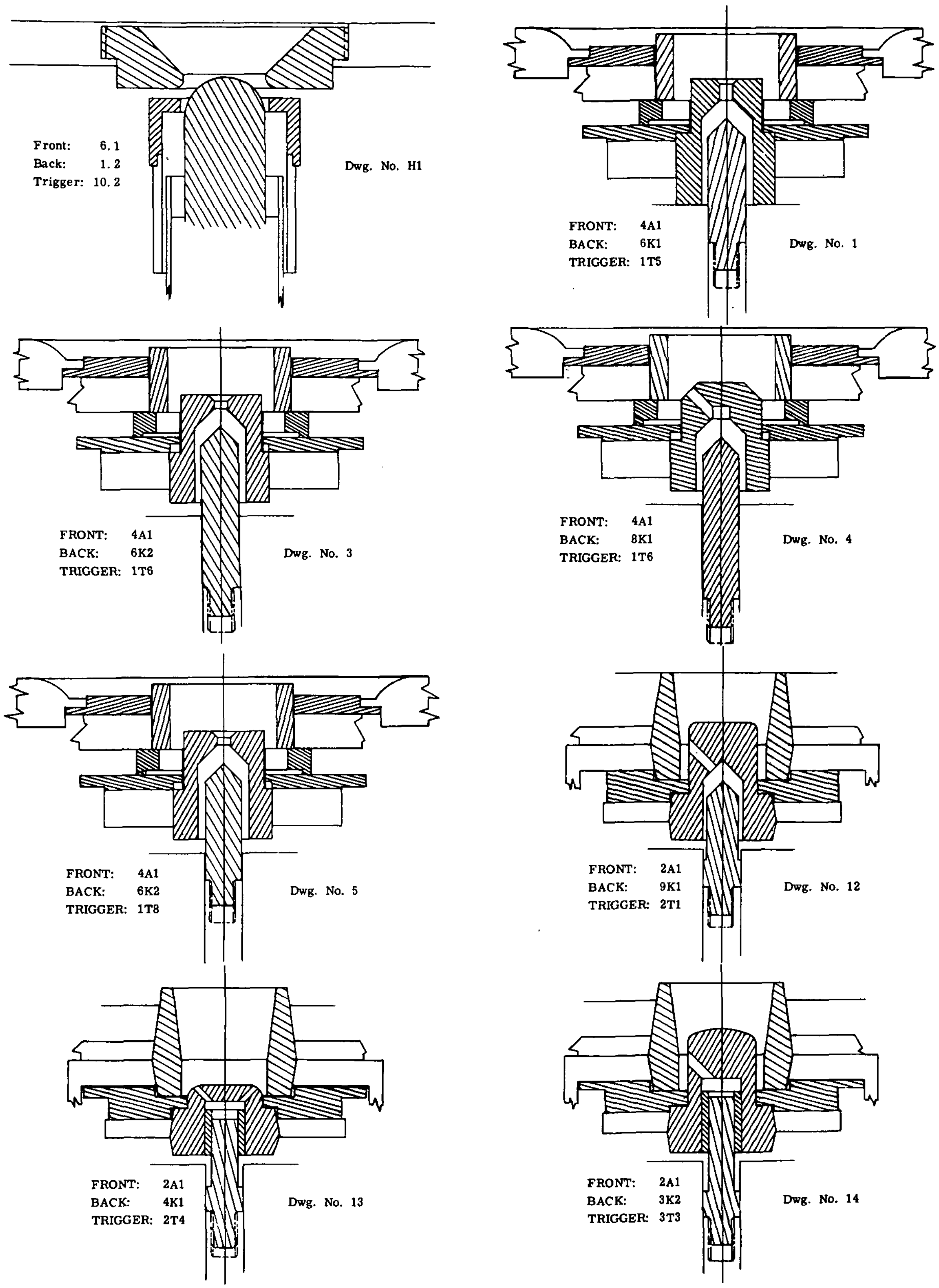

Figure 18. Some Variations in the Arc Chamber Geometry

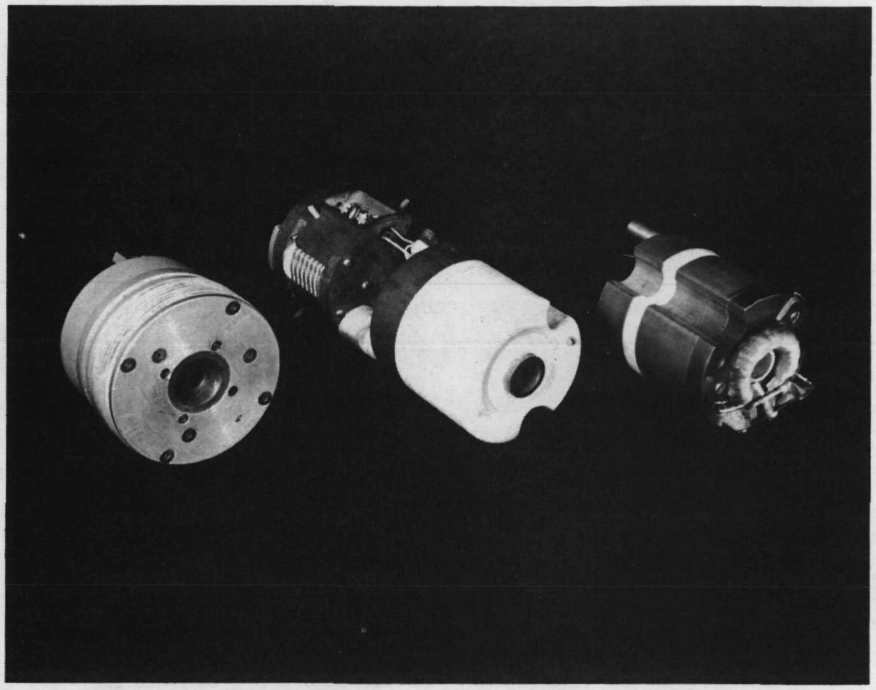

Figure 19. Revisions in the Thruster Design to Adapt to the New Mounting Arrangement

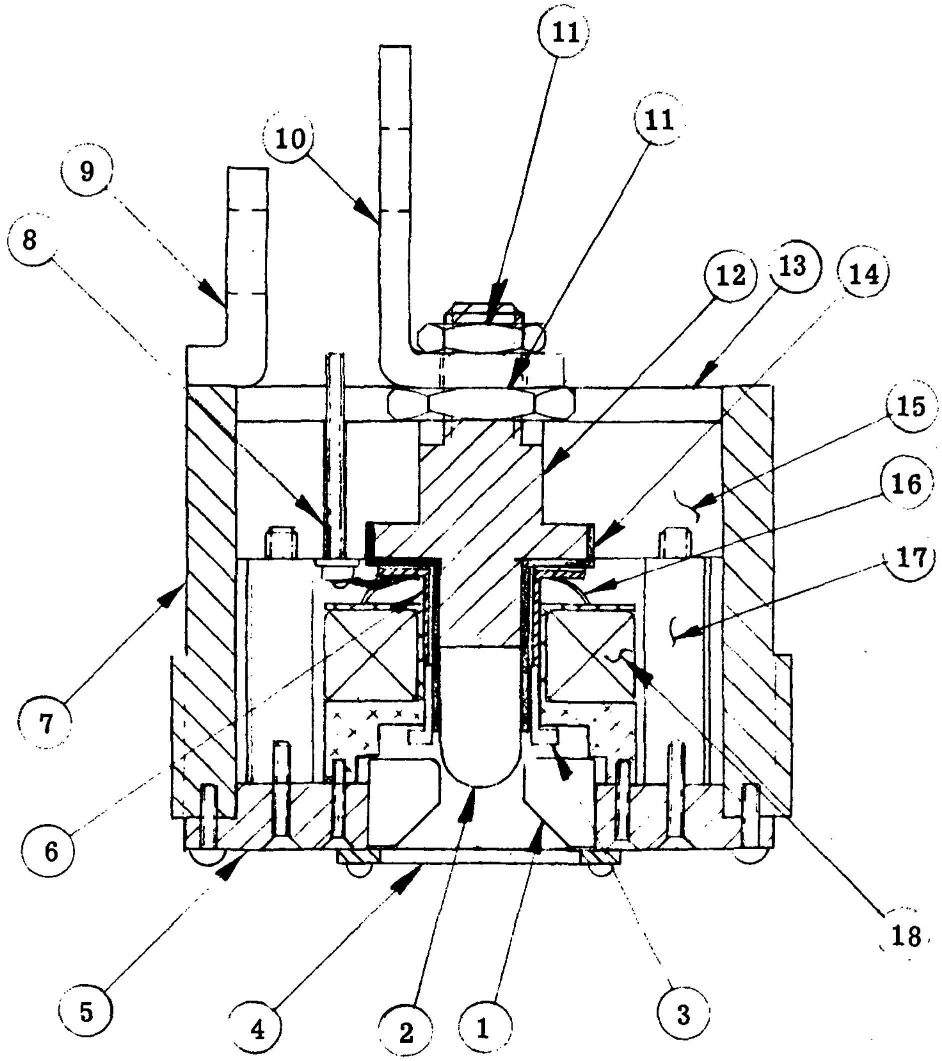

1. Anode Carbon Tip
2. Cathode Carbon Tip
3. Trigger Carbon Tip
4. Anode Tip Holder
5. Front Anode Connection
6. Magnetic Armature
7. Outside Anode Connection
8. Coil Connection
9. Anode Terminal
10. Cathode Terminal
11. Cathode Nuts
12. Cathode Copper Holder
13. Insulating Plate
14. Cathode Insulator
15. Insulator Block
16. Trigger Spring
17. Coil Holder
18. Coil Windings

Figure 20. Plasma Head No. 1
(Figure 33 of Reference 1)

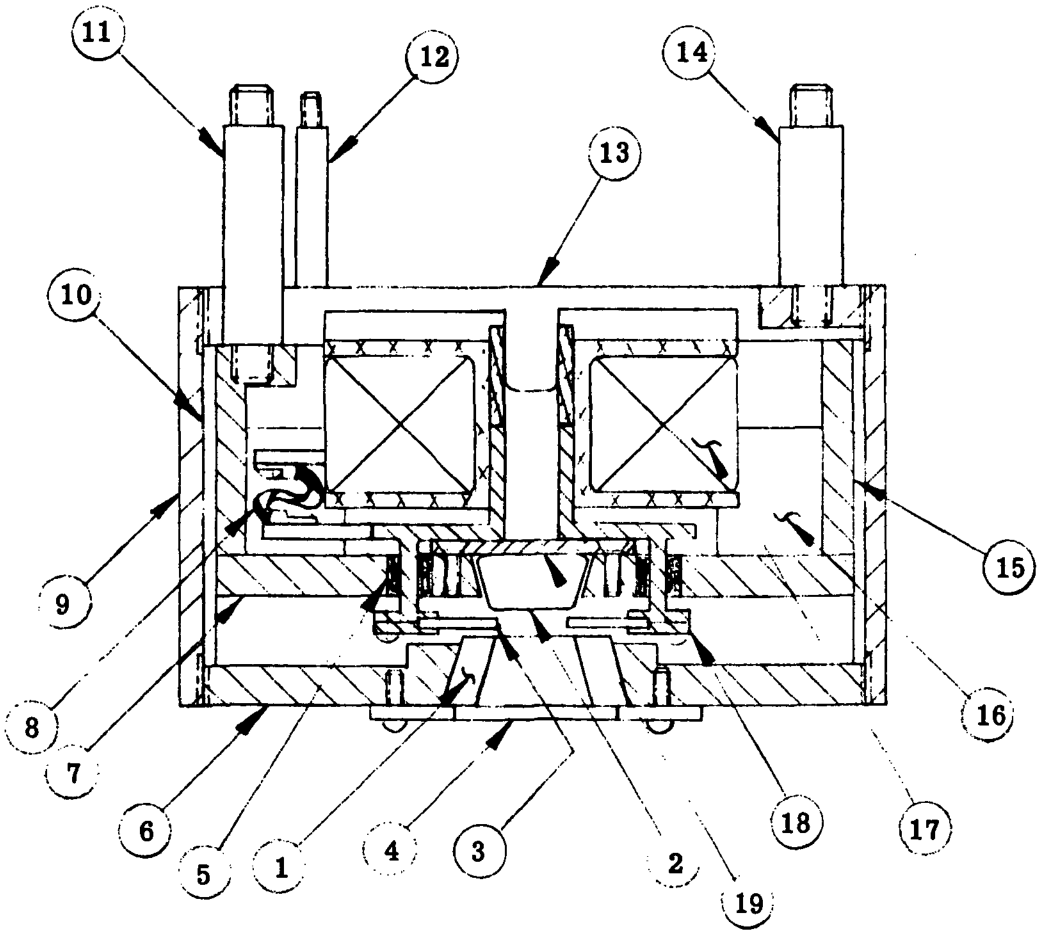

1. Anode Carbon Tip
2. Cathode Carbon Tip
3. Trigger Carbon Tip
4. Anode Holder
5. Insulator
6. Anode Front Plate
7. Cathode Front Plate
8. Trigger Connection
9. Anode Outside Connection
10. Insulator
11. Cathode Connection
12. Coil Connection
13. Insulator
14. Anode Connection
15. Cathode Outside Connection
16. Insulator
17. Coil
18. Insulating Support
19. Cathode Holder

Figure 21. Plasma Head No. 4
(Figure 35 of Reference 1)

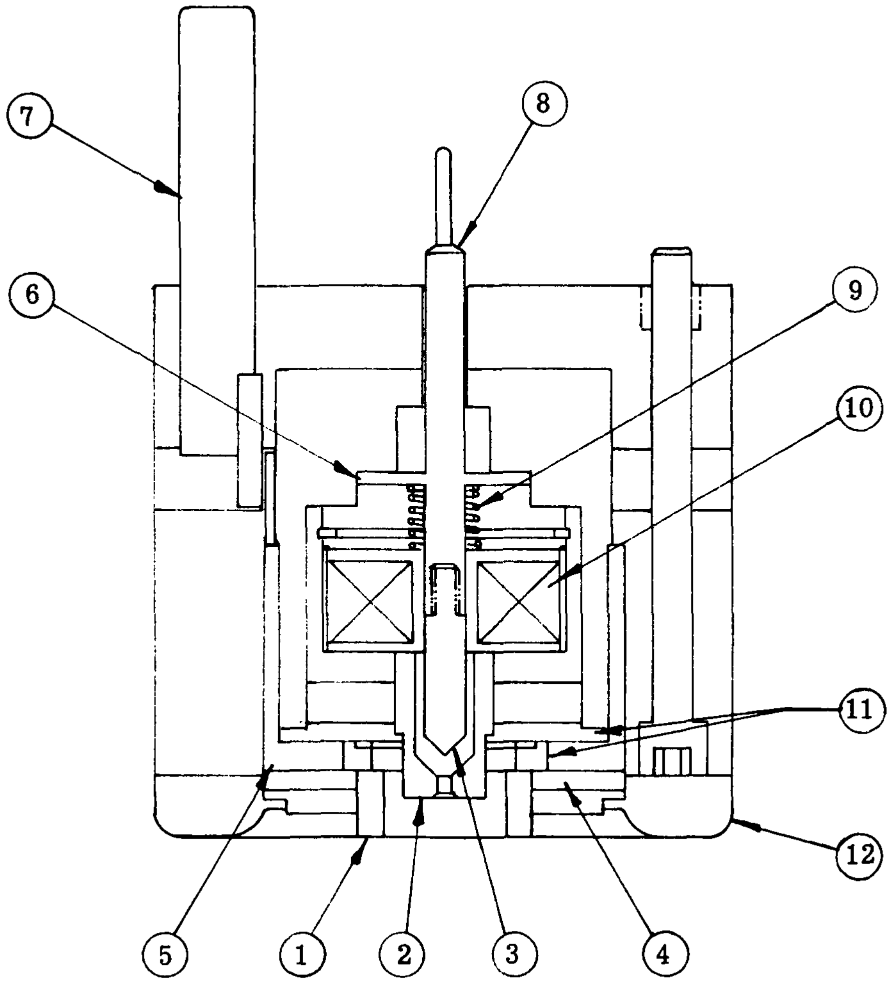

1. Anode Carbon Tip
2. Cathode Carbon Tip
3. Trigger Carbon Tip
4. Anode Tip Holder
5. Front Anode Connection
6. Magnetic Armature
7. Anode Terminal
8. Cathode Nuts
9. Trigger Spring
10. Coil Windings
11. Cathode Insulator
12. Front Plate (Teflon)

Figure 22. Typical Internal Arrangement of the Thruster (Head 20)

A final refinement has been the removal of Teflon insulator parts from the vicinity of the arc chamber to avoid the unexpectedly high evaporation rate of these parts even in areas some distance from the arc. Boron nitride is now used in more of these marginal locations.

Most of the progress made in changing the arc geometry to improve performance is concerned with increasing the radial gap between electrodes, improving the uniformity and collimation of the jet, and reducing the resistive losses in the electrodes. However, the design of electrodes that provide efficient thruster operation and permit continuous feeding requires that two separate, and in some respects conflicting, goals be satisfied. Designs that minimize resistive losses in the graphite tend to have a relatively thin layer of graphite backed by a metal conductor (as shown in Figures 20 and 21) and are unsuitable for electrode feeding. A compromise or a change in concept appears to be needed.

Previous work[2] has shown that the ablation rate for the anode depends strongly on the dimensions of the electrode, nearly vanishing if a heavy electrode is used; while the ablation rate of the cathode is essentially independent of its dimension. It can be inferred that the cathode spot heats the surface in a region so concentrated that the geometry of the surrounding electrode has little influence on local conditions. These observations led to the adoption of a configuration using an annular anode heavy enough to essentially eliminate vaporization, combined with cylindrical center cathode that can be fed axially as the material ablates.

A second reason for choosing a configuration using a center cathode is that a single cathode spot of high current density should offer a performance advantage if the spot can be stabilized near the center of the electrode. The advantage is obvious when the self-field model is used because the thrust depends on the natural log of the ratio of anode diameter to effective cathode diameter (the cathode spot diameter in the stabilized case). In addition, if the cathode spot is concentrated, a high pressure region is generated precisely at the point that cathode vapor is introduced to the arc. Expansion from this high pressure region provides a mechanism for the recovery of thermal energy and should result in improved efficiency. It is instructive to calculate the field strength and pressure in a concentrated cathode spot. These quantities are tabulated below for different values of arc current and cathode spot radius. The calculated values of magnetic field and pressure shown, are those that would result from electromagnetic forces alone.

Current (amps)	Cathode Spot Radius (mm)	Self Magnetic Field (gauss)	Pressure (atm)	Pressure (psi)
1000	10.0	200	0.0031	0.046
2000	10.0	400	0.0124	0.182
5000	10.0	1,000	0.0775	1.140
1000	1.0	2,000	0.3100	4.600
2000	1.0	4,000	1.2400	18.200
5000	1.0	10,000	7.7500	114.000

It is evident that significant recovery of thermal energy is possible in a stable concentrated cathode spot region. It seems to follow that the cathode jet should be directed downstream to enhance recovery of thermal energy and to assure a uniform, well-collimated jet. It is also concluded that better use is made of the thermal expansion effect if most of the propellant is vaporized at the cathode spot.

The above advantages of the central cathode geometry are opposed by a difficulty in finding a suitable arrangement for the triggering electrode. The arc starts more easily if the triggering electrode contacts the cathode; but in order to make the cathode feedable, some sort of unsymmetrical geometry would be required. The configurations tested so far are not suitable for electrode feeding.

Evidence that the desired thermal expansion effect is not being obtained in the present thruster designs is obtained from the appearance of the arc and plume and from an examination of the arc chamber parts following operation. Carbon deposits are found on the insulator upstream of the arc and on the anode itself which sometimes increases in weight during a test. This suggests that while carbon, which is evaporated from the cylindrical surface of the cathode, is accelerated axially by the self-field forces, a badly directed cathode jet converts thermal energy into radial velocity so that much of the material impinges on the cooler anode surface and is even carried upstream to the insulator. The thermal energy is not recovered, the heat of vaporization of this material is in effect lost, and the thruster life is jeopardized by carbon deposits on the insulator. Heavier carbon deposits are observed in the designs that have a small radial clearance between anode and cathode and a correspondingly poorer efficiency is also noted.

Early results from the photographic work being done for the AFOSR program show a strong arc pattern fairly uniformly distributed in the small annular clearance space between electrodes with a scattering of less bright spots on the cathode face. Most of the discharge appears to be across the smallest gap, and cathode spots seem to appear in many locations.

High speed motion pictures of early MPD thrusters of the steadily operating type show the cathode spot moving about in a region closer to the center of the cathode with a correlation clearly evident between cathode spot location and plume direction. The self-field forces were expected to pull the arc downstream to form a geometry of this type in the current designs, but this has apparently not occurred to the extent desired. The difficulty may be associated with the small radial clearance used between electrodes to enhance triggering of the pulsed arc. Correction of the present poor operating condition is considered one of the most important undertakings for future test programs.

Another problem of equal urgency is the high resistive losses in the present electrode designs. Current must enter the cathode through a metal fixture that clamps to the cylindrical surface. Normally, the clamping must occur some distance from the cathode tip to prevent direct arcing from the clamp to the anode, and to leave space for a triggering electrode. The result is a sizable resistive loss in the length of cathode between the clamp and the tip. From the standpoint of improving the arc impedance, it would be desirable to use a small cathode diameter to increase the ratio of anode to cathode radius. However, this would increase the resistive loss. Notice that there is a lower limit for cathode diameter for a given arc current. With smaller diameters, the potential gradient in the cathode would be greater than the potential gradient in the arc column, and the arc would prefer a more direct path to the clamping fixture. The cathode must therefore be relatively large, and the favorable ratio of anode to cathode radius must be obtained primarily by stabilizing the cathode spot at a central position or by increasing the anode diameter.

An alternate design being studied is one with conventional concentric electrodes, but with reversed polarity. In this case an effort is being made to obtain most of the propellant by vaporization of the central anode, while the cathode is operated as cool as possible. Advantages would be that the larger anode spot would permit reduced resistive losses in the center electrode, while a tungsten cathode would reduce resistive losses in the outer electrode. The triggering electrode could be in the cathode which would enhance the triggering action while leaving the anode a simple cylinder suitable for feeding. It may be that these gains can offset the advantages of the central cathode geometry, particularly if the stable concentration of the arc in a single cathode spot is not found to be practical. The configuration is expected to be of particular interest for cases where lower specific impulse is desired, because the large anode fall region losses can be used to vaporize the feedable electrode and provide initial heating of the propellant.

Another subject being studied is the choice of material for the electrodes. The material characteristic that is most urgently needed is high electrical conductivity. However, material choice can also affect performance in other ways and experiments have been initiated to explore possible gains due to additives which: a) improve electron emission from the cathode, thereby simplifying the triggering process and reducing cathode fall region losses; b) seed the propellant with a material that ionizes readily, thereby reducing resistive losses in the arc column; c) provide vaporization of the propellant at a particular rate so that the desired specific impulse is attained; or d) reduce the average molecular weight of the propellant to enhance thermal expansion effects. It is anticipated that the final configuration selected will utilize insulator feeding as well as electrode feeding so the choice of insulator material can affect the propellant properties as well as the choice of electrode material.

2.5 Discussion of Performance Data

The arc chamber geometries used during this test program are illustrated in Figures 18 and 22. Figure 18 shows the electrode configurations, while Figure 22 shows a typical configuration of the thruster body for holding the electrodes and actuating the triggering mechanism. These designs cover variations in the method of holding the electrodes, the electrode shapes, the arrangement of the triggering mechanism, and the insulator geometry. However, the most significant design variable from the standpoint of performance was found to be the radial gap between electrodes, or the ratio of the anode diameter to the cathode diameter. Comparatively small gaps were used in this group of tests in an effort to relieve a difficult arc triggering problem. It is convenient to think of the thruster designs as falling into two groups; those having very small electrode gaps (Drawings 12 and 13 of Figure 18 with $r_a/r_c = 1.13$ and 1.25), and those having a somewhat larger gap (Drawings 3, 4, and 1 of Figure 18 with $r_a/r_c = 1.33$ and 1.50). For comparison, the tests reported in Reference 1 were of a thruster having an anode and cathode of the same diameter (see Figure 20), but if the minimum gap is measured, an effective value of r_a/r_c equal to about 1.23 is obtained; so the design was nearly equivalent to the one shown in Drawing 12 of Figure 18. All of the designs used low voltage, contact-type triggering systems. The series was used in an initial exploration of the influence of electrode geometries on thruster performance and the ease with which the arc discharge can be triggered.

To maximize the number of designs evaluated, each thruster configuration was tested at only one pulse energy level (400 volts initial charge or about 4300 joules stored energy). This approach seems to be justified by the results reported in Reference 1 which show only minor variations in scaled performance with changes in the initial charge voltage. Results of the latest test series indicate that performance is strongly dependent on the thruster geometry, which encourages continued studies to find designs with improved performance.

During the course of the program, the testing technique was refined as deficiencies were discovered in the earlier procedures (see Sections 2.1 and 2.2). Some test points are therefore considered to be more accurate than others. Calculated performance is summarized in Table I for those test points considered to be of satisfactory accuracy. Results from Reference 1 for the case with 400 volts initial charge are also presented in the table for comparison. Test points after the preliminary data are arranged from top to bottom in order of increasing radial gap between electrodes.

The left third of the table identifies the test conditions giving the number of pulses in the series and the head configuration used (as identified in Figures 18 and 22). It should be noted that identical electrodes do not necessarily imply identical test conditions, as there are variations in the electrode material and in the design of the insulators used. The most conspicuous change in performance occurs when Teflon is substituted for boron nitride in an insulator located in the vicinity of the arc discharge. The use of Teflon insulator is denoted by an asterisk by the figure showing the amount of material consumed, and is generally accompanied by an increase in consumption and a reduction in specific impulse.

The center portion of the table presents information on overall thruster performance. The integrated value of electrical energy expended during the pulse is presented, followed by the average change in weight of arc chamber parts during a pulse and the total impulse produced by the thruster as measured by the torsional pendulum. Some of the values for propellant consumed are shown as negative, indicating that these parts gained in weight during the test series (an indication of carbon deposits). The last two columns give specific impulse and efficiency calculated from the measured quantities.

The right hand portion of the table shows estimated quasi-steady performance, or the performance that the thruster would have if it continued to operate at the conditions that exist while the voltage and current of the arc discharge are fairly constant. Since propellant flow rate and thrust are not measured during the pulse, these quantities must be estimated using an effective quasi-steady pulse duration, the selection of which involves a somewhat arbitrary judgment based on an examination of the oscilloscope traces of arc voltage and current. A constant value of 0.8 millisecond was used for the present program. The table also gives arc voltage, arc current, arc power, and arc impedance determined from estimated average voltage and current measured in the flat region of the oscilloscope trace. The mass flow rate and the thrust are determined from the propellant consumed per pulse and the total impulse respectively using the quasi-steady pulse duration. Finally, the last two columns give the "critical velocity" parameter $(J^2/\dot{m})$ and thrust constant (F/J^2) which are useful in comparing measured performance with theoretical models.

A number of observations can be made from these test results.

1. Although all of the tests were made with the same initial capacitor bank energy, test results cover a wide range of specific impulses and efficiencies. Apparently, the thruster design can have a strong influence on performance.

TABLE I

MEASURED PERFORMANCE

TEST CONDITIONS								THRUSTER PERFORMANCE**										ESTIMATED QUASI-STEADY PERFORMANCE								
			Electrode Geometry						Propellant Consumed Per Pulse (milligrams)									Arc Input Power								
1	2	3	4	5	6	7	8	9	10	11	12	13	14	15	16	17	18	19	20	21	22	23	24	25	26	27
							r_a/r_c	J	mg	mg	mg	mg	mg	mg	mg-sec	sec	%	m sec	V	kA	kW	m Ω	g/sec	g	$\frac{(kA)^2}{g/sec}$	$\frac{g}{(kA)^2}$
Ref. 1⊡	50	1⊙	H1	6.1◊	1.2‡	10.2†	1.23	3340	0.490	0.095	0.006	not used	*0.009	0.600	1669	2780	7.0	1.1	125	24.5	3060	5.10	0.545	1516	1101	2.52
1939-1973	34	20	13	2A1	4K1	2T4	1.13	2530	-0.026	0.694	-0.015	0.579	not used	1.232	986	800	1.5	0.8	95	24	2280	3.96	1.541	1232	373	2.14
2308-2407	100	20	14	2A1	3K2	3T3	1.25	3370	-0.118	-0.821	0.000	1.170	not used	1.873	990	529	0.7	0.8	100	22	2200	5.00	2.340	1239	206	2.56
1889-1938	50	20	12	2A1	9K1	2T1	1.25	2298	0.066	0.806	0.014	0.380	not used	1.266	1355	1070	3.1	0.8	110	20	2200	5.50	1.583	1695	252	4.24
3098-3148	51	20	4	4A1	8K1	1T6	1.33	2578	0.227	0.561	0.008	0.013	-0.031	0.778	2277	2927	12.4	0.8	110	22	2420	5.00	0.973	2845	498	5.89
3047-3097	48	20	3	4A1	6K2	1T6	1.33	2074	-0.029	0.792	0.025	-0.113	-0.027	0.648	2277	3514	18.5	0.8	110	22	2420	5.00	0.810	2845	598	5.89
3251-3301	51	20	5	4A1	6K2	1T8	1.33	2234	-0.049	0.753	0.033	-0.102	-0.027	0.608	1967	3234	11.3	0.8	120	22	2640	5.45	0.760	2460	637	5.09
2895-2945	51	20	1	4A1	6K1	1T5	1.50	2592	0.180	0.457	-0.006	0.132	*1.639	2.402	3450	1436	9.2	0.8	110	21	2310	5.24	3.000	4310	147	9.78
2945-2995	51	20	1	4A1	6K1	1T5	1.50	2896	0.124	0.608	0.012	0.671	-0.023	1.390	3174	2283	12.0	0.8	130	21	2730	6.20	1.749	3970	252	9.01
2996-3045	50	20	1	4A1	6K1	1T5	1.50	2544	0.252	0.552	-0.002	0.416	0.040	1.258	3623	2880	19.7	0.8	125	20	2500	6.25	1.572	4540	254	11.33
2844-2894	50	20	1	4A1	6K1	1T5	1.50	2638	0.126	0.504	-0.004	0.510	0.010	1.146	3312	2890	17.4	0.8	120	20	2400	6.00	1.432	4140	279	10.33

⊡ Ref. 1, Table IV, 400-volt series
⊙ Ref. 1, Figure 33
◊ Ref. 1, Figure 45, Model 6
‡ Ref. 1, Figure 44, Model 1
† Ref. 1, Figure 46, Model 10

*Teflon

**Does not include capacitor loss.

Column		
1	Shot Numbers	
2	Total Number of Pulses	
3	Head Number	
4	Electrode Geometry Dwg. No. (Fig. 18)	
5	Anode Identification	
6	Cathode Identification	
7	Trigger Identification	
8	Radius Ratio	(r_a/r_c)

Column		
9	Integrated Electrical Input Energy	(joules)
10	Outer Electrode Consumption/Pulse	(mg)
11	Center Electrode Consumption/Pulse	(mg)
12	Trigger Electrode Consumption/Pulse	(mg)
13	Disk Insulator Consumption/Pulse	(mg)
14	Ring Insulator Consumption/Pulse	(mg)
15	Total Consumption/Pulse	(mg)
16	Total Impulse	(mg-sec)
17	Specific Impulse	(sec)
18	Efficiency	(percent)

Column		
19	Duration of Quasi-Steady Regime	(m sec)
20	Volts	
21	Current (J)	(kA)
22	Power	(kW)
23	Arc Impedance	(m ohm)
24	Mass Flow ($\dot{m}$)	(g/sec)
25	Thrust (F)	(g)
26	$J^2/\dot{m}$	$(kA)^2/(g/sec)$
27	F/J^2	$(g/(kA)^2)$

The designs having the larger electrode gaps have efficiencies about twice as high as those reported in Reference 1.

2. The quasi-steady values of arc current and voltage correspond to an arc impedance of from 4 to 6 milliohms. Although some of the designs show an increase in impedance over values reported in Reference 1, this remains a relatively low range of values in consideration of the high resistive losses in the graphite electrodes. There is still a need for increased arc impedance or decreased electrode resistance.

3. In some cases, the insulator contributes a substantial fraction of the propellant. Note that the series of shots numbered 2895-2945 obtained over 70 percent of its propellant from the insulators, largely because of the introduction of a Teflon insulator in the vicinity of the electrodes. As a result, this unit ran at a specific impulse of around half of the average for the other three series using the same electrodes. This could provide a technique for controlling specific impulse. However, the lower efficiencies observed at reduced specific impulses suggests that the added propellant derived from insulator material may not be utilized as effectively by the arc as the material evaporated directly from the electrodes. This could result in less efficient energy transfer and nonuniformities in the jet velocity profile.

4. Visual observations of the arc and of cathode erosion patterns show that the cathode spot moves about on the cathode surface with a tendency to concentrate on the cylindrical outer surface of the electrode a large fraction of the time. One of the purposes of the design was to have the cathode spot concentrated near the center of the cathode, and in this respect, the thrusters did not perform as intended.

5. Performance appears to improve when the cathode diameter is small compared to the anode diameter. This would be expected for a case with the cathode spot moving freely over the electrode surface, and is predicted by both magnetic nozzle and self-field models of the thruster operation. The effect is evident in Figure 23, which shows the efficiency of the points of Table I plotted as a function of electrode diameter ratio. Although other design changes and a fair amount of test scatter are involved, the effect of electrode diameter ratio seems to dominate. These points are also shown plotted as a function of specific impulse in Figure 24.

6. Stable operation has been observed at higher values of specific impulse than would be expected from criteria developed for "starvation" instability in gas fed thrusters. The reason for this has not been determined.

Numbers by the test points identify the electrode geometry by drawing number as shown in Figure 18.

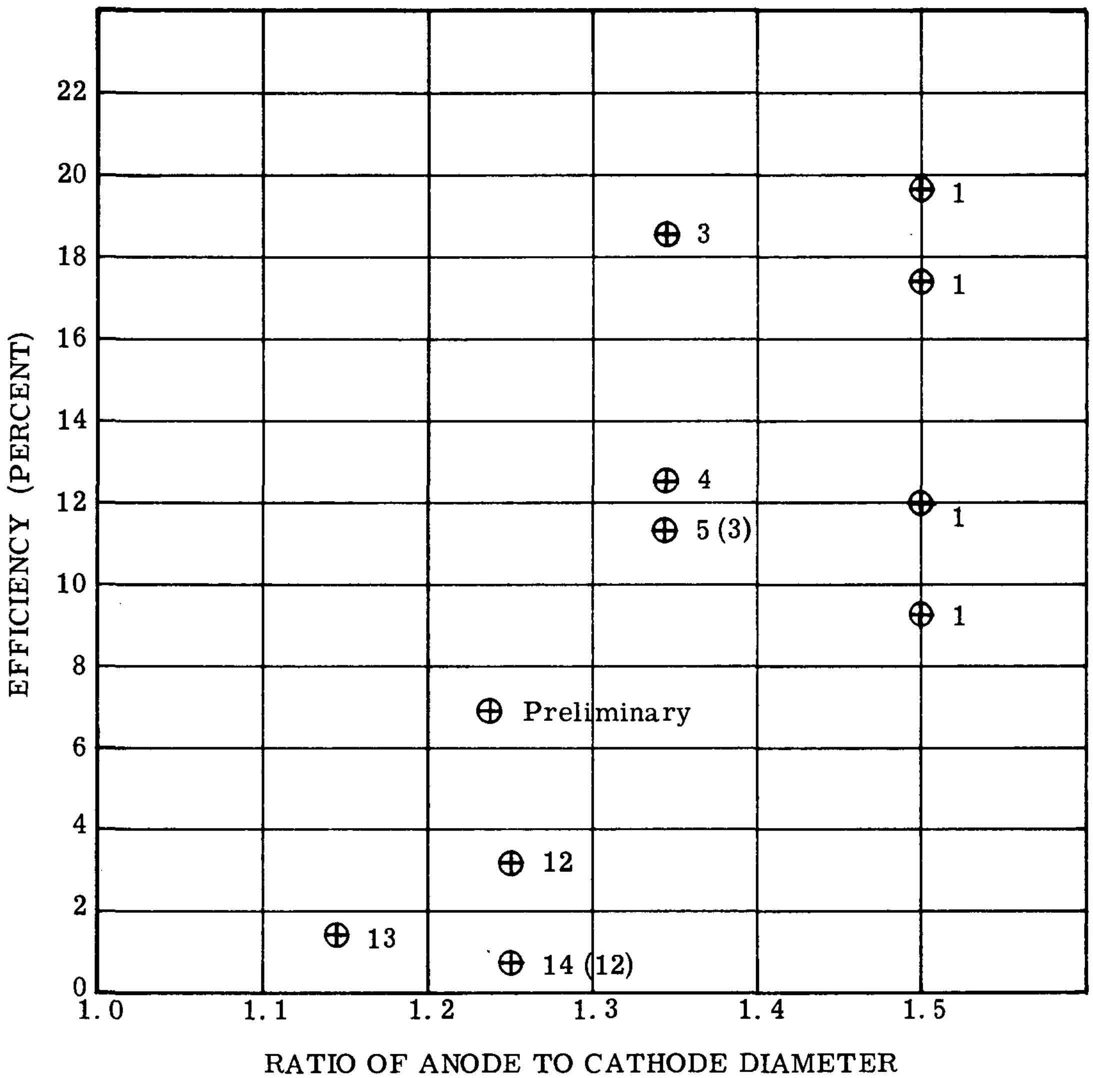

Figure 23. Thruster Efficiency Plotted as a Function of Electrode Diameter Ratio

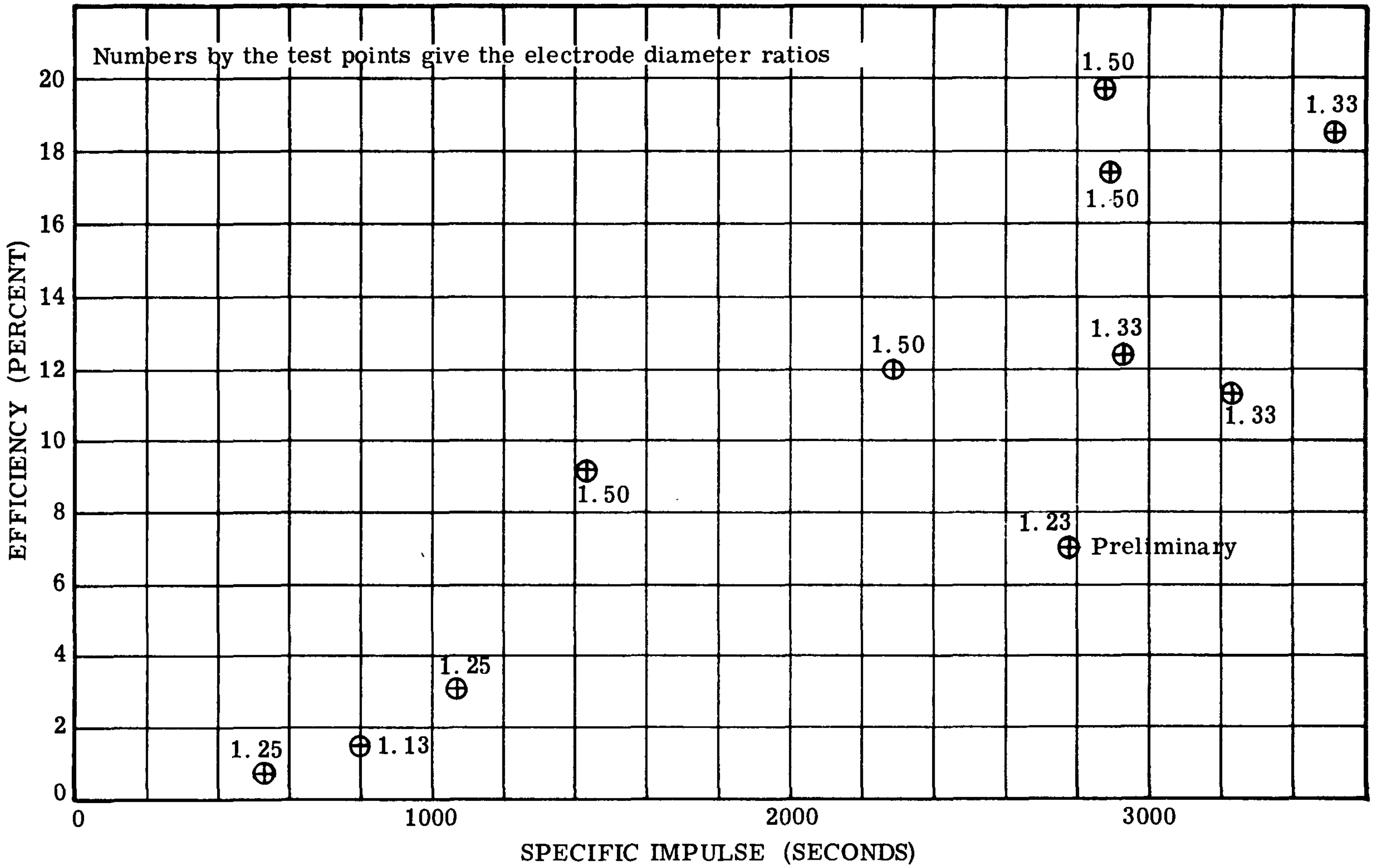

Figure 24. Thruster Efficiency Plotted as a Function of Specific Impulse

Some of the points regarding thruster performance are discussed in further detail in the paragraphs that follow.

Arc Impedance

The 4- to 6-milliohm discharge impedance observed in these tests is typical of a variety of MPD arcs in this current range,[5] but here it must be noted that some of the designs tested introduce internal resistances in their electrodes which may amount to around one-half of this value. The particular grade of carbon employed has a resistivity of about 0.0018 ohm-cm, which for the path lengths involved introduces an impedance comparable to the arc itself. This suspicion is supported by tests on a modified thruster specifically designed for shorter current paths through the carbon electrodes, where the average impedance is found to be about 2.2 milliohms. The true discharge impedance, therefore, may be as low as 2 or 3 milliohms in some cases.

The comparatively low net discharge impedance can probably be attributed to the very short electrode gaps that occur in these vacuum thrusters as a result of the failure of the cathode spot to concentrate at the center of the electrode. For example, for the early configuration used in Reference 1, the assumption of a discharge current path in reasonable agreement with the visual arc geometry yields a back emf from a 3×10^4 m/sec plasma stream of the order of only 10 volts for even the highest arc current studied. Clearly it would be desirable to increase this component of the arc impedance relative to the fixed losses in the circuit.

It should be noted, however, that the resistive losses in the electrodes have the same effect as ballast resistors and help to stabilize the arc. This may explain the ability of these designs to operate at high specific impulses without evidence of "starvation instability." If this is found to be the case, it will provide evidence that this type of instability can be controlled by a proper choice of circuit characteristics, and will suggest the design of circuits that provide this stabilization with reduced loss (if, indeed, the instability is found to have a serious effect on performance).

Thrust

A certain amount of judgment is required in estimating the thrust produced during a pulse since only total impulse is measured. For our purposes, we have assumed an effective quasi-steady period lasting 0.8 millisecond, and have divided this value into the measured impulse to obtain a nominal value of thrust. Figure 25 shows this value divided by the square of the quasi-steady arc current and plotted as a function of the electrode diameter ratio. For comparison, curves are shown for the theoretical self-field thrust for a case with all of the current entering the outer surface of the cathode, and for a case with uniform current density over the projected area of the cathode. It is interesting to

Numbers by the test points identify the electrode geometry by drawing number as shown in Figure 18.

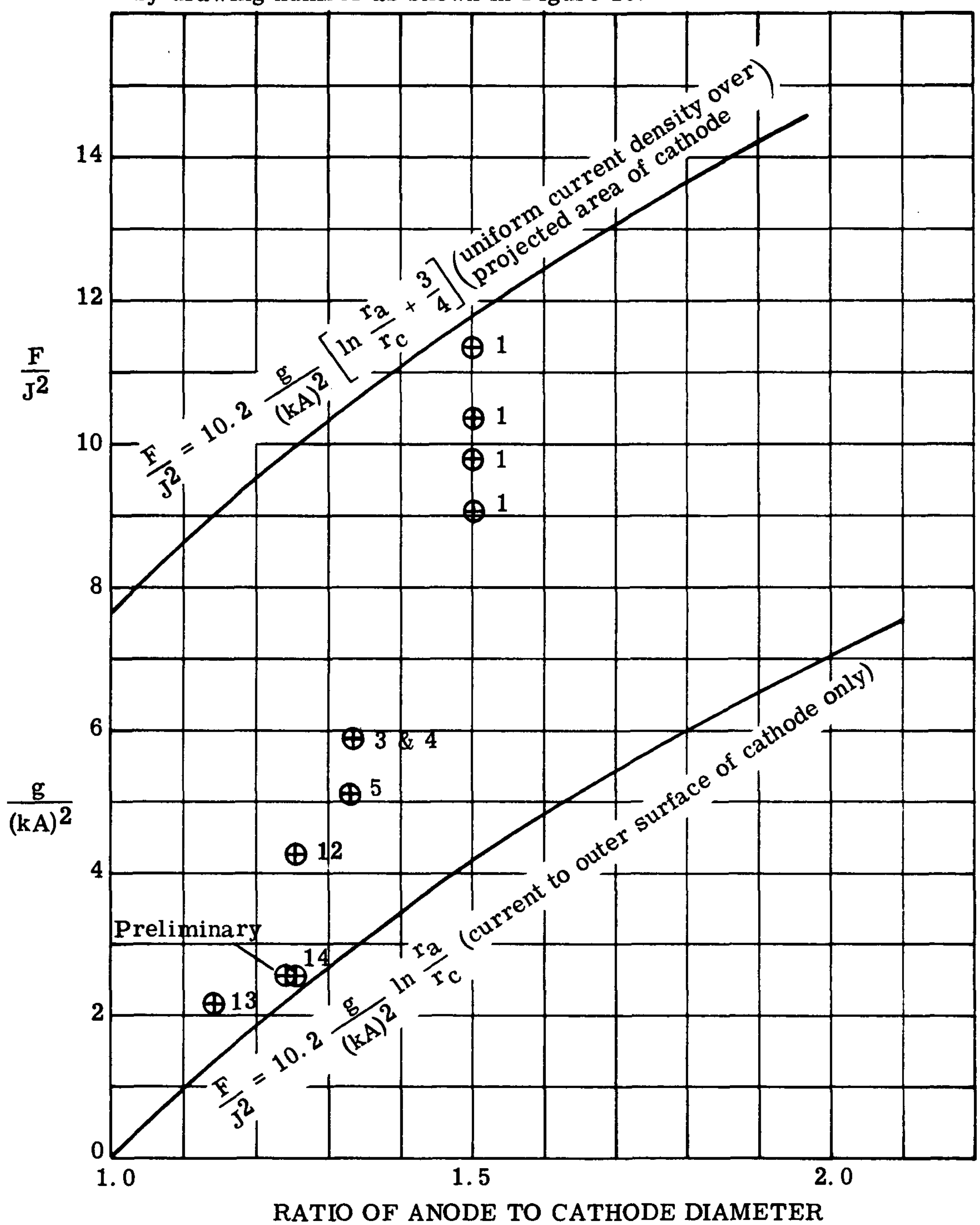

Figure 25. Comparison Between Measured Thrust and Thrust Predicted by the Self-Field Theory

note that the test points fall between these two theoretical lines with the lower curve approached at the low diameter ratios and the higher curve approached at the high diameter ratios. This suggests that if the radial gap between electrodes is small enough, the arc tends to remain in the small gap and is not drawn downstream. However, as the gap is increased, the arc geometry seems to improve rapidly. In principle, the upper curve can be exceeded if a stable arc spot can be established near the center of the inner electrode. However, in order to establish a uniform erosion pattern, it seems reasonable to consider the uniform current density line as a practical limit. It is likely that further gains in performance can be obtained by approaching the upper line more closely and by increasing the electrode diameter ratio.

Notice that the measurement of propellant mass consumed does not enter in determining the F/J^2 parameter, and errors in this measurement have no effect on Figure 25. Accordingly, these points show less scatter than appears in the plot of efficiency (Figures 23 and 24).

Efficiencies

The efficiency of energy transfer from the capacitor network to the discharge electrodes is over 50 percent and reasonable for a test installation, particularly in view of the modest quality of the capacitors themselves. It doubtless can be further improved both from that direction and by increasing the arc impedance to a better match with the line. The much lower efficiency of conversion of terminal energy into impulse has four obvious sources, and probably several others. The resistive losses in the carbon electrodes already discussed can consume over half of the terminal power in some cases, and probably return very little of it to the propellant stream. This loss can be reduced by redesign of the arc head, but there are limitations if a concept permitting feedable graphite electrodes is retained. Beyond this, one must look to the electrode surface losses, and to the thermodynamics and kinematics of the plasma flow.

The reduction of electrode losses by utilizing some of the surface energy flux to vaporize propellant is one of the main fortes of the vacuum MPD arc. Nevertheless, to take advantage of this, the energy flux to the electrode surfaces must be kept a small ratio of the energy deposited in the discharge column. As discussed earlier, a large gap appears to be desirable so that the sum of voltages developed by back emf and heating of the plasma stream is not small compared to the electrode falls.

Whatever input power remains after interior and surface electrode losses have been paid, divides in some fashion between streaming energy and the thermal capacities of the plasma. If the equipartition model is to be believed, some 56 e.v. is invested in the ionization of each carbon atom, and the same in its kinetic energy; what portion of the former can be recovered by expansion of the jet is speculative. If the equipartition mode is not applicable, the ratio of kinetic to thermal energy may be higher; but in either case, jet profile and divergence losses must still be allowed. Little is known about the plume pattern and composition at this time, but if more than one mass of particle is involved, e. g. polyatomic carbon, corresponding velocity groups must be expected, with the attendant losses in thrust.

Although a reduction in efficiency with decreasing specific impulse is considered normal for this type of thruster, the very low efficiencies shown in Figure 24 for low specific impulses require some discussion. For these thruster designs, low specific impulse is usually associated with rapid consumption of insulating material, which leads to the conjecture that the insulating material is not used as effectively as electrode vapor in the arc. Two possible explanations have been considered. The first is that electrodes introduce vapor directly into the hottest region of the arc foot while the insulating material may, to a large extent, bypass the arc in leaving the thruster. The second is that some portion of the boron nitride insulating material may be ejected as fine solid particles. The resultingly poor velocity distribution in the jet would have an adverse effect on performance. Further study of these possibilities is needed to determine if it is feasible to use insulating material in the propellant, or if ablation must be limited primarily to the electrodes alone.

3.0 CONCLUSIONS AND RECOMMENDATIONS

The major results of the work described in this report are listed below.

1. Improvements have been made in the test facility and particularly in the remote manipulators for removing and installing thrusters in an evacuated test chamber. It is now feasible to conduct fairly rapid tests of thrusters with consumable electrodes so that a reasonable number of geometries can be evaluated.

2. Performance appears to be a strong function of thruster design. Although all tests made during this program used the same capacitor bank energy, the efficiency and specific impulse obtained varied over a wide range. The better designs have an efficiency about twice as high as was reported in Reference 1, at the same specific impulse.

3. There is evidence that substantial improvements in performance can still be made by additional changes in design. The most promising areas are listed below.

   a. It was recognized in Reference 1 that the resistive losses in the graphite electrodes accounts for a large fraction of the electrical energy in each pulse. Although these losses have been reduced, they are still substantial. Their further reduction offers an opportunity for a significant improvement in efficiency.

   b. With low electrode diameter ratios, the arc discharge appears to concentrate on the cylindrical outer surface of the inner electrode rather than being carried to a central position as had been intended in the design. The result is poor performance as would be predicted by the self-field theory. An increase in the electrode diameter ratio improves performance rapidly, presumably because the arc assumes a more normal geometry with the arc attaching to the face rather than the sides of the inner electrode. In other words, the effective electrode diameter ratio increases more rapidly than the actual diameter ratio resulting in a dramatic improvement in performance as the radial gap between electrodes is increased. The largest diameter ratio tested was 1.5, so significant improvements may still be possible by further increasing the value.

   c. More carbon deposits are found on the anode and on the ring insulator when the radial gap between electrodes is small. It appears that the cathode jet, which is normally directed downstream into the plume, impinges on other parts of the thruster when the radial gap is small. This is an additional loss mechanism because the energy required to vaporize and accelerate this part of the graphite goes into heating other thruster parts and produces no thrust. The effect can be sizable, as over 20 percent of the material vaporized is redeposited in some cases. Performance should improve (and reliability should be enhanced) if geometries can be found that avoid the deposition of electrode vapor on other thruster parts.

d. It has been found that evaporation of insulating material can contribute a large fraction of the propellant. This material does not enter into the arc directly, may in some cases come off in the form of a fine dispersion of solid particles, and may not be accelerated as efficiently as the electrode vapor. Design of insulators with reduced erosion rates is expected to improve efficiency.

4. The triggering mechanism that initiates the arc discharge is a critical part of the design. Triggering is difficult in a vacuum arc because no gas is introduced in the arc chamber before the arc starts operating, and the use of high voltage for triggering should be avoided because the surfaces of insulators tend to become coated with a film of deposited electrode vapor. The large electrode gaps needed for efficient thruster operation require more effective low voltage triggering systems.

5. The low voltage, contact-type triggering systems used in this program have been found to work best if the main arc discharge is used as the cathode in the triggering discharge. Apparently, the main discharge is initiated when conditions necessary for electron emission are established on the cathode.

6. Stable arc operation has been observed at substantially higher values of specific impulse than would be expected from usual starvation instability criteria. The reason for this has not been established.

7. On the basis of the above results and experience to date, the following improvements and studies are recommended for continuing a systematic evaluation of quasi-steady thrusters with consumable electrodes.

   a. Refinements are needed to improve the accuracy of the test data, particularly the weight change of arc chamber parts that contribute to the propellant flow. These should include completion of the system for heating and weighing parts in a vacuum and development of a system for heating and weighing complete thrusters in a vacuum followed by tests using samples not exposed to the action of the arc to verify that unwanted effects on the measurement have been eliminated.

b. A study is needed to find ways of further improving thruster performance by reducing electrode resistive losses.

c. A study is needed to determine the effect of further increases in the radial gap between electrodes on performance, including efficiency, specific impulse, arc stability, ease of triggering, carbon deposition, plume geometry, and thruster life. Striking gains in efficiency have been obtained using this technique without approaching any clear-cut limitations

d. Continued study is needed to determine the effect on performance of variations in electrode shape, with special attention directed toward achieving a better concentration of the arc termination on the center electrode in a region near the thruster center line. Goals would include improved self-field action, better collimation of the jet, enhanced recovery of thermal energy, and reduced formation of carbon deposits on critical thruster parts. If successful, this approach would provide the same advantages as increased radial clearance with less penalty in terms of electrode resistance and difficult triggering.

e. Continued study is needed to obtain a better understanding of the nature of the cathode spot on a consumable electrode. Photographs show multiple spots on the face of the cathode which may be due to rapid movement of the arc attachment point or to parallel operation of a plurality of attachment points.

f. A study is needed to determine the effect on performance of electrode additives that could enhance cathode emission, increase ionization of gas in the discharge, control the specific impulse, or reduce the average molecular weight of the propellant.

g. A study is needed to determine if there are operating conditions that would cause "starvation" type instability to occur in this type of thruster; and, if possible, to establish why thrusters with consumable electrodes appear to be relatively free of this problem.

h. A study is needed to determine the effect on thruster performance of variations over a wide range of pulse duration, pulse shape, power density, and total pulse energy.

i. A study is needed of designs which permit continuous feeding of electrodes without an unacceptable sacrifice in performance. Approaches might include the use of electrodes of reverse polarity and/or the design of triggering electrodes that are not axially symmetrical.

j. Continued study is needed to find ways of improving the operation of the triggering electrode, with emphasis placed on satisfactory triggering of configurations that have a large radial gap between electrodes. An investigation should be included of the tolerance of the head to high triggering circuit voltage. It is expected that improvements in thruster design that reduce the deposition of a carbon film on the insulators will permit higher triggering voltages and larger electrode radial gaps to be used. This work should also include an examination of the feasibility of controlling the arc geometry by a judicious choice of the trigger electrode contact location and orientation.

REFERENCES

1. Ducati, A. C.; and Jahn, R. G.: Investigation of Pulsed Quasi-Steady MPD Arc Jet. NASA CR-111970, June 1971.

2. Ducati, A. C.; and Jahn, R. G.: Exploratory Electromagnetic Thruster Research, Phase III. NASA CR-66923, Feb. 1970.

3. Washburn, Edward W., ed: International Critical Tables of Numerical Data, Physics, Chemistry and Technology. Published for the National Research Council by McGraw Hill Book Company, 1933.

4. Dushman, S.; and Lafferty, J. M.: Scientific Foundations of Vacuum Technique. John Wiley and Sons, 1962.

5. Clark, K. E.; and Jahn, R. G.: Quasi-Steady Plasma Acceleration. AIAA Journal, 8, 216, 1970.

6. Malliaris, A. C.; John, R. R.; Garrison, R. L.; and Libby, D. R.: Quasi-Steady MPD Propulsion at High Power. NASA CR-111872, Feb. 1971.

UNCLASSIFIED

Security Classification

DOCUMENT CONTROL DATA - R & D

(Security classification of title, body of abstract and indexing annotation must be entered when the overall report is classified)

1. ORIGINATING ACTIVITY *(Corporate author)* Plasmadyne, a division of Geotel, Inc. 3839 South Main Street Santa Ana, California 92702	2a. REPORT SECURITY CLASSIFICATION UNCLASSIFIED 2b. GROUP NASA CR-112144

3. REPORT TITLE

QUSI-STEADY PLASMA ACCELERATORS

4. DESCRIPTIVE NOTES *(Type of report and inclusive dates)*

Scientific

5. AUTHOR(S) *(First name, middle initial, last name)*

Adriano C. Ducati

6. REPORT DATE	7a. TOTAL NO. OF PAGES	7b. NO. OF REFS
June 1972	41	6

8a. CONTRACT OR GRANT NO. NAS 1-10630 b. PROJECT NO. c. d.	9a. ORIGINATOR'S REPORT NUMBER(S) FR-062-10630 9b. OTHER REPORT NO(S) *(Any other numbers that may be assigned this report)*

10. DISTRIBUTION STATEMENT

11. SUPPLEMENTARY NOTES	12. SPONSORING MILITARY ACTIVITY National Aeronautics and Space Adm. Langley Research Center Hampton, Virginia 23365

13. ABSTRACT

Results are reported from a continued study of MPD thrusters operating in the quasi-steady mode and using electrode vapor as the propellant. Testing methods have been refined, and performance data is now available for a fairly wide range of thruster geometries. Performance was found to be strongly dependent on thruster geometry, with some designs showing approximately twice the efficiency obtained during the preceding contract period. The radial clearance between electrodes, the attachment point of the arc on the cathode, and the electrical resistance of the electrodes appear to be important design variables. As a result of the availability of reliable test data, the program is entering a rapid learning phase which could lead to further improvements in performance. The report presents test results, an analysis of these results and recommendations for continued work in the area.

DD FORM 1 NOV 65 1473

UNCLASSIFIED

Security Classification

14. KEY WORDS	LINK A		LINK B		LINK C	
	ROLE	WT	ROLE	WT	ROLE	WT
Arc Jet Environment						
Carbon and Graphite						
Carbon Vapor						
Electrode Erosion and Evaporation						
Electrolytic Capacitors						
Evaporation						
High Specific Impulse						
MPD Arc Jet						
MPD Test Environment						
Plasma Accelerator						
Plasma-Pulsed Accelerator						
Propulsion						
Pulse Networks						
Quasi-Steady						
Resonant Pulsing						
Sublimation						
Thrust Balance						
Vacuum Chambers						